Table 1 – Experimental groups.

Groups	Number of rats	Treatment	
		Infusion by Alzet pump	Transplantation
Fasudil+BMSC group	10	Fasudil	BMSC
Fasudil-only group	8	Fasudil	Saline
BMSC-only group	9	Saline	BMSC
Control group	10	Saline	Saline

The rats were randomly divided into four groups. The fasudil +BMSC group ($n=10$) received fasudil administration by Alzet osmotic mini pump and BMSC transplantation into the spinal cord. The fasudil-only group ($n=8$) received fasudil administration by Alzet pump and saline injection into the spinal cord. The BMSC-only group ($n=9$) received saline administration by Alzet pump and BMSC transplantation into the spinal cord. The control group ($n=10$) received saline administration by Alzet pump and saline injection into the spinal cord.

time period. The withdrawal threshold was calculated as the average of six consecutive tests.

Mechanical withdrawal thresholds in rat hind limbs were tested using a Dynamic Plantar Aesthesiometer (Ugo Basile), in which a mechanical stimulus was applied via an actuator filament (0.5 mm diameter), which under computer control applies a linear ramp 5.0 g/s to the plantar surface of the hind limb. The withdrawal threshold was calculated as the average of six consecutive tests. Both tests were performed 8 weeks after contusion. For comparison with baseline, we also performed both tests with normal rats ($n=31$).

4.5. *Anterograde labeling of corticospinal tracts with BDA, immunohistochemical, and histological assessment*

Nine weeks after contusion, the corticospinal tract (CST) was hemilaterally traced under halothane anesthesia with 2.0 μL biotinylated dextran amine (BDA, molecular weight: 10,000, 10% in 0.01 M PBS, Molecular Probes). A micro-glass pipette needle attached to a 2 μL Hamilton syringe was stereotaxically guided, and BDA was slowly injected into four sites in the sensorimotor cortex for the hind limb at a depth of 1 mm. The needle was left for an additional 1 min following each injection to minimize reflux.

Animals were subjected to trans-cardiac perfusion with 4% paraformaldehyde in PBS (pH 7.4) for 14 days after BDA injection. At the conclusion of the BDA infusion period (11 weeks after contusion), the spinal cords were dissected and immersed overnight in 4% paraformaldehyde, then stored in 20% sucrose in PBS. The spinal cords were cut into 20 mm lengths (10 mm rostral and 10 mm caudal from the lesion site) and embedded in OCT compound (Tissue Tek, Sakura Finetechnical, Tokyo, Japan). These blocks were sectioned in the sagittal plane (section thickness=25 μm) using a cryostat. We mounted a set of serial sections on a total of eight poly-L-lysine-coated slides (Matsunami, Tokyo, Japan) for each animal. Each slide contained six sliced sections at 200 μm intervals, and the sections for each slide were offset by 25 μm from the previous slide in the set. By this method, we were able to cover approximately 1200 μm of the lesion at 25 μm intervals in these eight slides. We processed the slides for histological or immunohistochemical staining.

To evaluate lesion size, one slide from one animal was stained with cresyl violet. The three slices showing the greatest damage were selected from one slide, and cavity size was determined with Photoshop 5.5 software (Adobe, San Jose, CA). Mean lesion size values for each group were calculated using these three lesions size values for each animal, and mean size comparisons were performed among the four groups.

In order to identify cell populations and characterize the cellular response, sections were immunolabeled with one or more antibodies. Anti-green fluorescent protein (GFP, rabbit polyclonal antibody, 1: 1600, Molecular Probes) was used to identify grafted rat BMSCs. The number of surviving transplanted cells and the localization of the cells were evaluated. Double immunohistochemical staining was performed with GFP plus either mouse anti-glial fibrillary acidic protein (GFAP, 1:400, Sigma, St. Louis, MO) or mouse anti-GSTπ (1:400, BD Pharmingen, Franklin Lakes, NJ), or mouse anti-NeuN (1:400; Chemicon) to evaluate transdifferentiation of BMSCs into astrocytes, oligodendrocytes, and neurons, respectively. After reacting with primary antibodies, the sections were incubated with Alexa Fluor 488-conjugated anti-mouse or anti-rabbit IgG (Molecular Probes) and with Alexa Fluor 594-conjugated anti-mouse or anti-rabbit IgG (Molecular Probes).

To evaluate residual and regenerative fibers, rabbit anti-neurofilament polyclonal antibody (1:800, Sigma) and rabbit anti-serotonin (5-HydroxyTryptamine, 5-HT) polyclonal antibody (1:5000, Sigma) were used for pan-nerve fibers. After reacting with primary antibodies, the sections were incubated with Alexa Fluor 488-conjugated anti-rabbit IgG (Molecular Probes) to detect positive signals. The numbers of immunoreactive fibers that traversed the virtual lines perpendicular to the central axis of the grafts were counted at three locations: the lesion site, 2.5 mm rostral from the lesion site, and 2.5 mm caudal from the lesion site.

For anterograde labeling of CSTs with BDA, sections were incubated with Alexa Fluor 594-conjugated streptavidin (1:800; Molecular Probes). The distance from the end of the labeled axons to the edge of the lesion site and the number of CST axons at the lesion site were measured.

The fluorescent signals were observed by fluorescence microscopy, ECLIPSE E600 (Nikon, Tokyo, Japan), and DP71 (Olympus, Tokyo, Japan). To maintain blinding in this histological study, observers were kept unaware of treatment groups.

4.6. *Statistical analysis*

Data were evaluated by multiple comparisons between groups. For histological studies, one-way ANOVA followed by the Bonferroni/Dunn *post hoc* test was used. For the 9-week locomotor scale, repeated-measures ANOVA followed by the Turkey-Kramer *post hoc* test was used. For fractional BBB score at each time point, one-way ANOVA followed by the Turkey-Kramer *post hoc* test was used. Data are presented as mean values±SEM. Differences were considered statistically significant at $^{*}p<0.05$.

Acknowledgments

Fasudil was kindly provided by Asahi Kasei Corporation (Tokyo, Japan). This research was supported by grant-in-aid for Japanese scientific research grant 19591715.

REFERENCES

Ackery, A., Robins, S., Fehlings, M.G., 2006. Inhibition of Fas-mediated apoptosis through administration of soluble Fas receptor improves functional outcome and reduces posttraumatic axonal degeneration after acute spinal cord injury. J. Neurotrauma 23, 604–616.

Akiyama, Y., Radtke, C., Kocsis, J.D., 2002. Remyelination of the rat spinal cord by transplantation of identified bone marrow stromal cells. J. Neurosci. 22, 6623–6630.

Alvarez-Dolado, M., Pardal, R., Garcia-Verdugo, J.M., Fike, J.R., Lee, H.O., Pfeffer, K., Lois, C., Morrison, S.J., Alvarez-Buylla, A., 2003. Fusion of bone-marrow-derived cells with Purkinje neurons, cardiomyocytes and hepatocytes. Nature 425, 968–973.

Amano, M., Fukata, Y., Kaibuchi, K., 2000. Regulation and functions of Rho associated kinase. Exp. Cell Res. 261, 44–51.

Azizi, S.A., Stokes, D., Augelli, B.J., DiGirolamo, C., Prockop, D.J., 1998. Engraftment and migration of human bone marrow stromal cells implanted in the brains of albino rats- Similarities to astrocyte grafts. Proc. Natl. Acad. Sci. U. S. A. 95, 3908–3913.

Baptiste, D.C., Fehlings, M.G., 2006. Pharmacological approaches to repair the injured spinal cord. J. Neurotrauma 23, 318–334.

Basso, D.M., Beattie, M.S., Bresnahan, J.C., 1995. A sensitive and reliable locomotor rating scale for open field testing in rats. J. Neurotrauma 12, 1–21.

Chan, C.C., Wong, A.K., Liu, J., Steeves, J.D., Tetzlaff, W., 2007. ROCK inhibition with Y27632 activates astrocytes and increases their expression of neurite growth-inhibitory chondroitin sulfate proteoglycans. Glia 55, 369–384.

Chen, Q., Long, Y., Yuan, X., Zou, L., Sun, J., Chen, S., Perez-Polo, J.R., Yang, K., 2005. Protective effects of bone marrow stromal cell transplantation in injured rodent brain: synthesis of neurotrophic factors. J. Neurosci. Res. 80, 611–619.

Chopp, M., Zhang, X.H., Li, Y., Wang, L., Chen, J., Lu, D., Lu, M., Rosenblum, M., 2000. Spinal cord injury in rat: treatment with bone marrow stromal cell transplantation. Neuroreport 11, 3001–3005.

Chopp, M., Li, Y., 2002. Treatment of neural injury with marrow stromal cells. Lancet Neurol. 1, 92–100 Review.

Deng, W., Obrocka, M., Fischer, I., Prockop, D.J., 2001. In vitro differentiation of human stromal cells into early progenitors of neural cells by conditions that increase intracellular cyclic AMP. Biol. Biophys. Res. Commun. 282, 148–152.

Dezawa, M., Kanno, H., Hoshino, M., Cho, H., Matsumoto, N., Itokazu, Y., Tajima, N., Yamada, H., Sawada, H., Ishikawa, H., Mimura, T., Kitada, M., Suzuki, Y., Ide, C., 2004. Specific induction of neuronal cells from bone marrow stromal cells and application for autologous transplantation. J. Clin. Invest. 113, 1701–1710.

Dickson, B.J., 2001. Rho GTPases in growth cone guidance. Curr. Opin. Neurobiol. 11, 103–110.

Dubreuil, C.I., Winton, M.J., McKerracher, L., 2003. Rho activation patterns after spinal cord injury and the role of activated Rho in apoptosis in the central nervous system. J. Cell Biol. 162, 233–243.

Hara, M., Takayasu, M., Watanabe, K., Noda, A., Takagi, T., Suzuki, Y., Yoshida, J., 2000. Protein kinase inhibition by fasudil hydrochloride promotes neurological recovery after spinal cord injury in rats. J. Neurosurg. 93 (1 Suppl.), 94–101.

He, Y, Xu, H, Liang, L, Zhan, Z, Yang, X, Yu, X, Ye, Y, Sun, L., 2008. Antiinflammatory effect of Rho kinase blockade via inhibition of NF-kappaB activation in rheumatoid arthritis. Arthritis Rheum. 58, 3366–3376.

Hess, D.C., Abe, T., Hill, W.D., Studdard, A.M., Carothers, J., Masuya, M., Fleming, P.A., Drake, C.J., Ogawa, M., 2004. Hematopoietic origin of microglial and preivascular cells in brain. Exp. Neurol. 186, 134–144.

Himes, B.T., Neuhuber, B., Coleman, C., Kushner, R., Swanger, S.A., Kopen, G.C., Wagner, J., Shumsky, J.S., Fischer, I., 2006. Recovery of function following grafting of human bone marrow-derived stromal cells into the injured spinal cord. Neurorehabilitation Neural. Repair 20, 278–296.

Hofstetter, C.P., Schwarz, E.J., Hess, D., Widenfalk, J., El Manira, A., Prockop, D.J., Olson, L., 2002. Marrow stromal cells from guiding strands in the injured spinal cord and promote recovery. Proc. Natl. Acad. Sci. U. S. A. 99, 2199–2204.

Isele, N.B., Lee, H.S., Landshamer, S., Straube, A., Padovan, C.S., Plesnila, N., Culmsee, C., 2007. Bone marrow stromal cells mediate protection through stimulation of PI3-K/Akt and MAPK signaling in neurons. Neurochem. Int. 50, 243–250.

Kamada, T., Koda, M., Dezawa, M., Yoshinaga, K., Hashimoto, M., Koshizuka, S., Nishio, Y., Moriya, H., Yamazaki, M., 2005. Transplantation of bone marrow stromal cell-derived Schwann cells promotes axonal regeneration and functional recovery after complete transection of adult rat spinal cord. J. Neuropathol. Exp. Neurol. 64, 37–45.

Kim, B.J., Seo, J.H., Bubien, J.K., Oh, Y.S., 2002. Differentiation of adult bone marrow stem cells into neuroprogenitor cells in vitro. Neuroreport 13, 1185–1188.

Koda, M., Okada, S., Nakayama, T., Koshizuka, S., Kamada, T., Nishio, Y., Someya, Y., Yoshinaga, K., Okawa, A., Moriya, H., Yamazaki, M., 2005. Hematopoietic stem cell and marrow stromal cell for spinal cord injury in mice. Neuroreport 16, 1763–1767.

Kopen, G.C., Prockop, D.J., Phinney, D.G., 1999. Marrow stromal cells migrate throughout forebrain and cerebellum, and they differentiate into astrocytes after injection into neonatal mouse brains. Proc. Natl. Acad. Sci. U. S. A. 96, 10711–10716.

Koshizuka, S., Okada, S., Okawa, A., Koda, M., Murasawa, M., Hashimoto, M., Kamada, T., Yoshinaga, K., Murakami, M., Moriya, H., Yamazaki, M., 2004. Transplanted hematopoietic stem cells from bone marrow differentiate into neural lineage cells and promote functional recovery after spinal cord injury in mice. J. Neuropathol. Exp. Neurol. 63, 64–72.

Kubo, T., Yamashita, T., 2007. Rho-ROCK inhibitors for the treatment of CNS injury. Recent Patents CNS Drug Discov. 2, 173–179.

Lee, J.B., Kuroda, S., Shichinohe, H., Yano, S., Kobayashi, H., Hida, K., Iwasaki, Y., 2004. A pre-clinical assessment model of rat autogeneic bone marrow stromal cell transplantation into the central nervous system. Brain Res. Brain Res. Protoc. 14, 37–44.

Liu, X.Z., Xu, X.M., Hu, R., Du, C., Zhang, S.X., McDonald, J.W., Dong, H.X., Wu, Y.J., Fan, G.S., Jacquin, M.F., Hsu, C.Y., Choi, D.W., 1997. Neuronal and glial apoptosis after traumatic spinal cord injury. J. Neurosci. 17, 5395–5406.

Lu, P., Jones, L.L., Tuszynski, M.H., 2005. BDNF-expressing marrow stromal cells support extensive axonal growth at sites of spinal cord injury. Exp. Neurol. 191, 344–360.

Monnier, P.P., Sierra, A., Schwab, J.M., Henke-Fahle, S., Mueller, B.K., 2003. The Rho/ROCK pathway mediates neurite growth-inhibitory activity associated with the chondroitin sulfate proteoglycans of the CNS glial scar. Mol. Cell. Neurosci. 22, 319–330.

Mueller, B.K., Mack, H., Teusch, N., 2005. Rho kinase, a promising drug target for neurological disorders. Nat. Rev. Drug Discov. 4, 387–398.

Neuhuber, B., Timothy Himes, B., Shumsky, J.S., Gallo, G., Fischer, I., 2005. Axon growth and recovery of function supported by

human bone marrow stromal cells in the injured spinal cord exhibit donor variations. Brain Res. 1035, 73–85.
Nishio, Y., Koda, M., Kamada, T., Someya, Y., Kadota, R., Mannoji, C., Miyashita, T., Okada, S., Okawa, A., Moriya, H., Yamazaki, M., 2007. Granulocyte colony-stimulating factor attenuates neuronal death and promotes functional recovery after spinal cord injury in mice. J. Neuropathol. Exp. Neurol. 66, 724–731.
Ohta, M., Suzuki, Y., Noda, T., Ejiri, Y., Dezawa, M., Kataoka, K., Chou, H., Ishikawa, N., Matsumoto, N., Iwashita, Y., Mizuta, E., Kuno, S., Ide, C., 2004. Bone marrow stromal cells infused into the cerebrospinal fluid promote functional recovery of the injured rat spinal cord with reduced cavity formation. Exp. Neurol. 187, 266–278.
Ramer, LM, Borisoff, JF, Ramer, MS., 2004. Rho-kinase inhibition enhances axonal plasticity and attenuates cold hyperalgesia after dorsal rhizotomy. J Neurosci. 24, 10796–10805.
Rossignol, S., Schwab, M., Schwartz, M., Fehlings, M.G., 2007. Spinal cord injury: time to move? J. Neurosci. 27, 11782–11792 Review.
Sanchez-Ramos, J., Song, S., Cardozo-Pelaez, F., Hazzi, C., Stedeford, T., Willing, A., Freeman, T.B., Saporta, S., Janssen, W., Patel, N., Cooper, D.R., Sanberg, P.R., 2000. Adult bone marrow stromal cells differentiate into neural cells in vitro. Exp. Neurol. 164, 247–256.
Satoh, S., Toshima, Y., Ikegaki, I., Iwasaki, M., Asano, T., 2007. Wide therapeutic time window for fasudil neuroprotection against ischemia-induced delayed neuronal death in gerbils. Brain Res. 1128, 175–180.
Sauerzweig, S., Munsch, T., Lessmann, V., Reymann, K.G., Braun, H., 2009. A population of serum deprivation-induced bone marrow stem cells (SD-BMSC) expresses marker typical for embryonic and neural stem cells. Exp. Cell Res. 315, 50–66.
Shiokawa, M, Yamaguchi, T, Narita, M, Okutsu, D, Nagumo, Y, Miyoshi, K, Suzuki, M, Inoue, T, Suzuki, T., 2007. Effects of fasudil on neuropathic pain-like state in mice. Nihon Shinkei Seishin Yakurigaku Zasshi 27, 153–159 Japanese.
Someya, Y., Koda, M., Dezawa, M., Kadota, T., Hashimoto, M., Kamada, T., Nishio, Y., Kadota, R., Mannoji, C., Miyashita, T., Okawa, A., Yoshinaga, K., Yamazaki, M., 2008. Reduction of cystic cavity, promotion of axonal regeneration and sparing, and functional recovery with transplanted bone marrow stromal cell-derived Schwann cells after contusion injury to the adult rat spinal cord. J. Neurosurg. Spine 9, 600–610.
Song, S., Kamath, S., Mosquera, D., Zigova, T., Sanberg, P., Vesely, D.L., Sanchez-Ramos, J., 2004. Expression of brain natriuretic peptide by human bone marrow stromal cells. Exp. Neurol. 185, 191–197.
Sung, J.K., Miao, L., Calvert, J.W., Huang, L., Louis Harkey, H., Zhang, J.H., 2003. A possible role of RhoA/Rho-kinase in experimental spinal cord injury in rat. Brain Res. 959, 29–38.
Terada, N., Hamazaki, T., Oka, M., Hoki, M., Mastalerz, D.M., Nakano, Y., Meyer, E.M., Morel, L., Petersen, B.E., Scott, E.W., 2002. Bone marrow cells adopt the phenotype of other cells by spontaneous cell fusion. Nature 416, 542–545.
Wennersten, A., Meier, X., Holmin, S., Wahlberg, L., Mathiesen, T., 2004. Proliferation, migration, and differentiation of human neural stem/progenitor cells after transplantation into a rat model of traumatic brain injury. J. Neurosurg. 100, 88–96.
Woodbury, D., Schwarz, E.J., Prockop, D.J., Black, I.B., 2000. Adult rat and human bone marrow stromal cells differentiate into neurons. J. Neurosci. Res. 15, 364–370.
Woodbury, D., Reynolds, K., Black, I.B., 2002. Adult bone marrow stromal stem cells express germline, ectodermal, endodermal, and mesodermal genes prior to neurogenesis. J. Neurosci. Res. 69, 908–917.
Wright, K.T., El Masri, W., Osman, A., Roberts, S., Chamberlain, G., Ashton, B.A., Johnson, W.E., 2007. Bone marrow stromal cells stimulate neurite outgrowth over neural proteoglycans (CSPG), myelin associated glycoprotein and Nogo-A. Biochem. Biophys. Res. Commun. 354, 559–566.
Wu, S., Suzuki, Y., Ejiri, Y., Noda, T., Bai, H., Kitada, M., Kataoka, K., Ohta, M., Chou, H., Ide, C., 2003. Bone marrow stromal cells enhance differentiation of cocultured neurosphere cells and promote regeneration of injured spinal cord. J. Neurosci. Res. 72, 343–351.
Yano, S., Kuroda, S., Shichinohe, H., Seki, T., Ohnishi, T., Tamagami, H., Hida, K., Iwasaki, Y., 2006. Bone marrow stromal cell transplantation preserves gammaaminobutyric acid receptor function in the injured spinal cord. J. Neurotrauma 23, 1682–1692.
Ying, Q.L., Nichols, J., Evans, E.P., Smith, A.G., 2002. Changing potency by spontaneous fusion. Nature 416, 545–548.
Yoshihara, H., Shumsky, J.S., Neuhuber, B., Otsuka, T., Fischer, I., Murray, M., 2006. Combining motor training with transplantation of rat bone marrow stromal cells does not improve repair or recovery in rats with thoracic contusion injuries. Brain Res. 1119, 65–75.
Zhu, H., Mitsuhashi, N., Klein, A., Barsky, L.W., Weinberg, K., Barr, M.L., Demetriou, A., Wu, G.D., 2006. The role of the hyaluronan receptor CD44 in mesenchymal stem cell migration in the extracellular matrix. Stem Cells 24, 928–935.

Tohoku J. Exp. Med., 2009, **219**, 139-143

Running Exercise for Short Duration Increases Bone Mineral Density of Loaded Long Bones in Young Growing Rats

Yoshinobu Hagihara,[1*] Arata Nakajima,[1*] Satoshi Fukuda,[2] Sumio Goto,[1*] Haruzo Iida[2] and Masashi Yamazaki[1]

[1]Department of Orthopaedic Surgery, Chiba University Graduate School of Medicine, Chiba, Japan
[2]International Space Radiation Laboratory, National Institute of Radiological Sciences, Chiba, Japan

Running exercise is an effective therapy for the prevention of osteoporosis; however, appropriate duration of exercise has not been determined. We therefore investigated the effect of exercise duration on bone mineral density (BMD) and systemic bone metabolism using young growing rats. Fifteen 8-week-old female Wistar rats were divided into three groups according to running load: control group (no running), short duration (30 min/day) and long duration (180 min/day), and animals ran on a treadmill 5 days per week over an 8-week period. BMD of the tibia was measured using peripheral quantitative computed tomography, and serum levels of tartarate-resistant acid phosphatase (TRAP), a bone resorption marker and alkaline phosphatase (ALP), a bone formation marker were measured to know whether the treadmill exercise would affect systemic bone metabolism. Short-duration running exercise (30 min/day) caused a significant increase in BMD of the metaphyseal trabecula ($p < 0.05$) with a reduction of serum TRAP levels ($p < 0.01$) and an increase in serum levels of calcium ($p < 0.05$) and phosphorus ($p < 0.01$). Conversely, long-duration exercise (180 min/day) significantly reduced BMD of the diaphyseal and metaphyseal cortex and that of the diaphyseal trabecula with a significant reduction of serum ALP levels and a significant increase in serum phosphorus. These findings suggest that short-duration exercise may increase BMD through suppression of bone resorption, whereas long-duration exercise may reduce BMD through suppression of bone formation. Exercising for short duration but not prolonged exercise is recommended to increase BMD of loaded long bones. ——— running exercise; duration; bone mineral density; bone formation; bone resorption.

Tohoku J. Exp. Med., 2009, **219** (2), 139-143.

Current strategies for the prevention of osteoporosis focus on maximizing the accumulation of bone mass early in life during growth and maturation, and minimizing bone loss later in life (Kulak and Bilezikian 1998; Rozenberg et al. 1999; Iwamoto et al. 2009). Achieving the maximum bone mass at skeletal maturity is the best protection against osteoporotic fractures (Matkovic et al. 1990; Iwamoto et al. 2009). Because physical activity during childhood and adolescence may be one of the most important determinants of peak bone mass, exercise should be emphasized during this period (Iwamoto et al. 2009).

Several studies have demonstrated that moderate exercise in the pre-menopausal period, including puberty, increases bone mineral density (BMD) (Myburgh et al. 1990, 1993; Prior et al. 1990; Welten et al. 1994; Friedlander et al. 1995; Goto et al. 1995); however, excessive exercise in this period reduces BMD (Yingling et al. 2001; Barry and Kohrt 2008). Using young growing rats, we previously verified the effects of moderate exercise in the form of running on a treadmill at a speed of 15 m/min for 30 min per day, over an 8-week period, on BMD of the long bones. We determined that the appropriate exercise frequency to increase BMD of the long bones was 4 to 5 days per week (Hagihara et al. 2005). However, the optimal combination of exercise frequency and duration to maximize BMD has not been established.

The purpose of the present study was to examine the effects of running for short (30 min) and long (180 min) durations on BMD of the loaded long bones and bone metabolic markers in young growing rats. These rats were subject to loading of a moderate magnitude (treadmill running at a speed of 15 m/min) over an 8-week period.

Received August 4, 2009; revision accepted for publication August 20, 2009. doi:10.1620/tjem.219.139

*Present Addresses: Y.H., Department of Orthopaedic Surgery, Joto Social Insurance Hospital, Tokyo; A.N., Department of Orthopaedic Surgery, Chiba Aoba Municipal Hospital, Chiba; S.G., Waku Orthopaedic Clinic, Chiba.

Correspondence: Masashi Yamazaki, M.D., Ph.D., Department of Orthopaedic Surgery, Chiba University Graduate School of Medicine, 1-8-1 Inohana, Chuo-ku, Chiba 260-8670, Japan.

e-mail: masashiy@faculty.chiba-u.jp

Table 1. Mean body weights of rats at the start and end of the experiment, and weight gained during the experimental period.

Group	Start (g)	End (g)	Weight gained (g)
Control	212.0 ± 11.40	263.0 ± 16.14	66.8 ± 6.14
SD	214.6 ± 8.65	267.4 ± 16.94	68.4 ± 9.40
LD	210.4 ± 11.95	258.2 ± 13.41	62.2 ± 6.98

SD, short duration; LD, long duration.

Materials and Methods

Animals and housing conditions

Fifteen 6-week-old female Wistar rats, with a mean weight of 156.8 g, were purchased. Animals were housed five to a cage and kept in a room with a temperature of 22 ± 2°C; relative humidity, 55 ± 5%; and a 12-h dark and light cycle. They were allowed free access to drinking water and commercial solid food (BM-1; Funabashi Farm, Funabashi, Japan) containing 1.2% calcium.

Running exercise and procedures

A treadmill device (Shinano, Tokyo, Japan) was used to provide a running load to the rats. Rats were pre-exercised for 2 weeks to habituate them to the device and to determine suitable running conditions, as described later. The rats were then divided into the following groups: control (no running); short duration (30 min/day) load (SD); long duration (180 min/day) load (LD). Each group consisted of five animals. The running load was initiated when the rats were 8 weeks old. The running conditions were determined according to our previous publications (Hagihara et al. 2000, 2005). All rats ran at a treadmill speed of 15 m/min, a speed at which they ran voluntarily and did not drop out. Animals ran 5 days per week (running on Monday through Wednesday and Friday through Saturday, resting on Sunday and Thursday), over a period of 8 weeks. This study was approved by the ethics committee of Chiba University.

Measured items

Body weights and food intakes of the rats were measured every day before and after running to check for untoward findings arising from the load. To determine whether the treadmill load affected the 4-day estrous cycle of the rats, vaginal smears were collected at 11 : 00 a.m. daily for 5 days in the first and third weeks, and for 10 consecutive days from the sixth week of the experiment. The collected vaginal smears were stained with Giemsa, and cells were observed under a light microscope.

The rats were killed under anesthesia using chloroform. The blood was collected from the posterior vena cava after celiotomy and centrifuged at 3,000 rpm. The serum was frozen and stored at −20°C. Concentrations of total serum calcium (Ca), phosphorus (P), and tartarate-resistant acid phosphatase (TRAP) were determined by the o-cresol phthalein complexone (OCPC), molybdenum blue, and p-nitrophenylphosphate (PNPP) substrate method, respectively.

Tibiae were collected and fixed in 70% ethanol. Measurements of BMD and the bone cross-sectional area were performed using peripheral quantitative computed tomography (pQCT) (voxel: 148 mm, 18.9 mm; XCT-960A) (Norland and Stratec, Germany). In this system, values of less than 395 and more than 690 mg/cm^3 are regarded as trabecular BMD and cortical BMD, respectively. The trabecular BMD was measured at a position 3 mm from the center of the cartilage plate image in the proximal epiphysis of the tibia. Cortical BMD was measured 12 mm away from the respective cartilage plate.

Table 2. Concentration of calcium and phosphorus in the serum.

Group	Ca (mg/dl)	*P* (mg/dl)
Control	10.58 ± 0.48	9.06 ± 0.87
SD	13.80 ± 2.22*	11.48 ± 1.15**
LD	11.58 ± 1.87	10.92 ± 1.13*

SD, short duration; LD, long duration.
*Significantly different from controls, $p < 0.05$; **$p < 0.01$.

Table 3. Concentration of TRAP and ALP in the serum.

Group	TRAP (IU/ml)	ALP (IU/ml)
Control	39.04 ± 5.91	359.0 ± 60.8
SD	26.16 ± 3.12**	331.4 ± 64.5
LD	31.98 ± 6.71	250.6 ± 56.7*

SD, short duration; LD, long duration.
*Significantly different from controls, $p < 0.05$; **$p < 0.01$.

Statistical analyses

Differences between groups were determined by an ANOVA. Where differences existed, the Fisher protected least significant difference test was used to determine significance. A value of $p < 0.05$ was considered statistically significant. All values were expressed as means ± S.D.

Results

There were no significant differences in food intake between groups. Also, there were no alterations or differences in the estrous cycle among the groups. The increase in body weight of group SD was higher than that of the other two groups, but no significant differences were seen among the groups (Table 1).

Regarding serum biochemistry, there was a significant increase in serum calcium values in group SD, and in serum phosphorus values in groups SD and LD compared to the control group (Table 2). The ALP level, a bone formation marker, was significantly decreased in group LD, but not altered in group SD (Table 3). It was of great interest that the TRAP level, a bone resorption marker, was significantly reduced in group SD (Table 3).

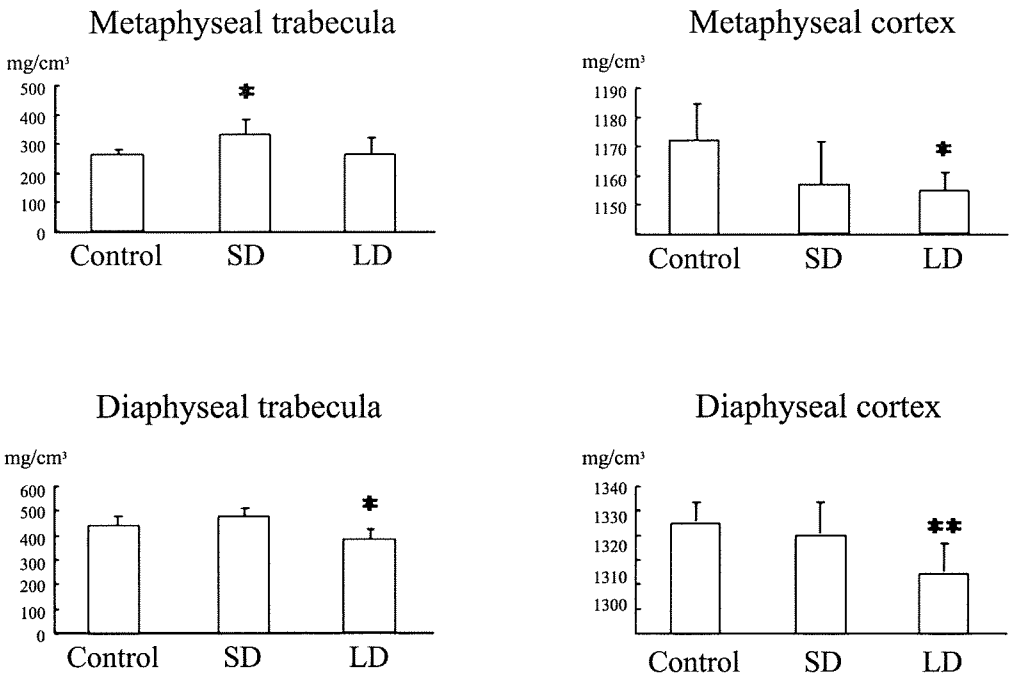

Fig. 1. BMD of the metaphyseal trabeculae and cortex of the tibia, and that of the diaphyseal trabeculae and cortex. Thirty-minute exercise periods (short duration) significantly increased BMD of the metaphyseal trabecula compared to the control (no running) group. In contrast, 180-minute periods (long duration) significantly reduced BMD of the diaphyseal and metaphyseal cortex, and that of the diaphyseal trabecula compared to controls. *Significantly different from controls, $p < 0.05$; **$p < 0.01$. SD, short duration; LD, long duration.

Most importantly, BMD of the metaphyseal trabecula of the tibia was significantly increased in group SD, but no significant differences were noted between group LD and the control group (Fig. 1). BMD of the metaphyseal cortex was lower in groups SD and LD than in the control group; however, the reduction was only significant in group LD (Fig. 1).

In contrast, BMD of the diaphyseal trabecula was not altered between group SD and the control group, while it was reduced significantly in group LD (Fig. 1). Similarly, there were no significant differences in BMD of the diaphyseal cortex between group SD and the control group, but there was a significant decrease in that of group LD (Fig. 1).

Discussion

In the present study, we examined the effect of exercise duration on BMD of the tibia. Running for a short duration significantly decreased TRAP levels in the serum, leading to a significant increase in BMD of the metaphyseal trabecula. Conversely, extended running significantly reduced serum ALP levels, resulting in a significant decrease in BMD of the metaphyseal cortex and that of the diaphyseal trabecula and cortex.

Several studies investigating the relationship between exercise and BMD have shown that moderate exercise increases BMD, while excessive exercise such as marathon running induces a decrease in BMD (Myburgh et al. 1990, 1993; Prior et al. 1990; Welten et al. 1994; Friedlander et al. 1995; Goto et al. 1995). Although we did not precisely define optimum running conditions for maximizing BMD, we did demonstrate clearly that running for a short duration (30 min/day) was more effective at increasing BMD of the metaphyseal trabecula of the tibia than running for a longer duration (180 min/day). Previously, we found no changes in adrenal gland weights after rats were subjected to a running exercise load of 15 m/min (Fukuda et al. 2002), the speed used in the present study. In our prior study, the 8-week-old male rats were run for 90 min/day for 35 days and we inferred that this regimen did not subject the rats to significant stress. Thus the speed of 15 m/min was considered to be a moderate load for the 8-week-old rats used in the present study. Though the durations tested were different from the prior study, we considered the overall stress to which the animals were exposed to be similar to the previous study.

It is of great significance that running for a short duration increased BMD of the metaphyseal trabecula but not BMD of the cortical bone. We previously reported that BMD of the metaphyseal trabecula in rat tibiae subjected to a moderate running load was significantly higher than that of controls. There were no significant differences in BMD of the diaphyseal cortex (Hagihara et al. 2005), consistent with the results presented here. Iwamoto et al. (2000) previously demonstrated that treadmill exercise significantly increased proximal tibial cancellous bone volume but not tibial shaft cortical bone area in young growing rats, supporting our results that showed the differential effect of running exercise on the trabecular and cortical bone.

In this study, running for a short duration increased BMD of the metaphyseal trabecula of the tibia and decreased serum TRAP levels but did not alter the ALP levels. This suggests that exercising for a short duration may have a negative effect on bone catabolism, with no significant effects on bone anabolism. Recently, Iwamoto et al. (2005) showed that treadmill exercise increases cortical and cancellous bone mass of the tibia as a result of increased bone formation and decreased bone resorption in young and adult rats. In addition, they revealed that treadmill exercise prevents cancellous bone loss at the tibia as a result of suppressed bone resorption, and increases bone mass of the tibia and mechanical strength of the femur as a result of suppressed bone resorption and increased bone formation in osteopenic rats after ovariectomy (Iwamoto et al. 2005). Although neither short nor long duration exercise increased serum ALP levels in the present study, these findings, at least in part, support our results. Given that the mechanism by which the BMD was increased was due to inhibition of bone resorption and not promotion of bone formation, running may have more of an effect on trabecular bones than cortical bones because trabecular bones contain more osteoclasts.

Also noteworthy was the observation that prolonged exercise significantly diminished BMD both for trabecular and cortical bone in the tibial diaphysis. Considering that prolonged exercise significantly reduced serum ALP levels, it seems conceivable that the BMD would be reduced more significantly in trabeculae than cortices because trabeculae contain more osteoblasts; however, BMD of the cortex (both metaphyseal and diaphyseal) was significantly reduced. We speculate two possible explanations for this inconsistency. Like trabecular osteoblasts, periosteal osteoprogenitor cells are considered to have high levels of ALP activity in young growing rats (Mizuno et al. 2006; Park et al. 2007). Thus, it is possible that periosteal osteoprogenitor cells rather than trabecular osteoblasts were affected more strongly by the long duration exercise-induced decrease in bone formation, resulting in significant loss of BMD of the cortex. Another is the issue that we may not able to simply correlate decrease in serum ALP levels with decrease in bone formation because we did not measure bone-specific ALP. To establish mechanisms by which long duration exercise reduced BMD of the cortex, analyses for bone-specific markers and dynamic parameters by bone histomorphometry will be necessary.

Exercise has an effect on calciotropic hormones. In rats, it promotes a positive calcium balance and increases skeletal mass, largely as a result of an increase in 1,25-dihydroxyvitamin D_3 and enhancement of intestinal calcium absorption (Yeh et al. 1989; Yeh and Aloia 1990). Consistent with this observation, in the present study animals exercised for a short period exhibited a significant increase in serum calcium levels; however, those run for a prolonged duration showed no significant hormonal changes. This suggests that running for a short period increases serum 1,25-dihydroxyvitamin D_3 levels and intestinal absorption of calcium, which in turn, decreases absorption of calcium from bone, resulting in inhibition of bone resorption. Iwamoto et al. (2004) investigated effects of treadmill exercise on calciotropic hormones in young growing rats, and demonstrated that exercise increases the serum 1,25-dihydroxyvitamin D_3 level and decreases the serum parathyroid hormone level, resulting in an increase in bone mass with stimulation of longitudinal bone growth, especially at weight bearing sites. Although the serum calcium level was not altered in exercised rats and controls in their study, these results appear to support our results and explanation to why short duration exercise-induced decrease in serum calcium levels lead to the decrease in bone resorption.

A limitation of the present study is the lack of bone (including both trabecular and cortical bones) histomorphometric analyses. Therefore, the alternations in local bone formation and bone resorption, cellular activities and bone architecture in the tibia remain uncertain. Further studies are essential to establish the effects of exercise duration on these dynamic parameters in loaded long bones such as the tibia.

In conclusion, short duration exercise increased BMD of the tibia while prolonged exercise did not. The mechanism by which exercise for a short duration increases BMD may be inhibition of systemic bone resorption. Prolonged exercise may reduce BMD through suppression of systemic bone formation. To increase the peak bone mass during the pre-menopausal period exercise duration must be neither too short nor too long. The optimal duration and load in humans, however, remains to be established.

References

Barry, D.W. & Kohrt, W.M. (2008) BMD decreases over the course of a year in competitive male cyclists. *J. Bone Miner. Res.*, **23**, 484-491.

Friedlander, A.L., Genant, H.K., Sadowsky, S., Byl, N.N. & Gluer, C.C. (1995) A 2-year program of aerobics and weight training enhances bone mineral density of young women. *J. Bone Miner. Res.*, **10**, 574-585.

Fukuda, S., Iida, H., Hyakutake, S. & Yan, X. (2002) Preventive effects of running exercise on bones in heavy ion particle irradiated rats. *J. Radiat. Res.*, **43** (suppl), S233-238.

Goto, S., Hyakutake, S. & Shigeta, H. (1995) Significance and effects of athletics for prevention of osteoporosis (in Japanese). *Osteoporosis Japan*, **3**, 110-118.

Hagihara, Y., Fukuda, S., Goto, S., Hasegawa, S., Iida, H., Yamagata, M., Saisu, T. & Moriya, H. (2000) Effects of continuous running exercise on bone mineral density in young rats (in Japanese). *Osteoporosis Japan*, **8**, 220-223.

Hagihara, Y., Fukuda, S., Goto, S., Iida, H., Yamazaki, M. & Moriya, H. (2005) How many days per week should rats undergo running exercise to increase BMD? *J. Bone Miner. Metab.*, **23**, 289-294.

Iwamoto, J., Sato, Y., Takeda, T. & Matsumoto, H. (2009) Role of sport and exercise in the maintenance of female bone health. *J. Bone. Miner. Metab.*, Apr. **7**. (Epub ahead of print).

Iwamoto, J., Shimamura, C., Takeda, T., Abe, H., Ichimura, S., Sato, Y. & Toyama, Y. (2004) Effects of treadmill exercise on bone mass, bone metabolism, and calciotropic hormones in young growing rats. *J. Bone Miner. Metab.*, **22**, 26-31.

Iwamoto, J., Takeda, T. & Sato, Y. (2005) Effect of treadmill exercise on bone mass in female rats. *Exp. Anim.*, **54**, 1-6.

Iwamoto, J., Yeh, J.K. & Aloia, J.F. (2000) Effect of deconditioning on cortical and cancellous bone growth in the exercise trained young rats. *J. Bone Miner. Res.*, **15**, 1842-1849.

Kulak, C.A. & Bilezikian, J.P. (1998) Osteoporosis: preventive strategies. *Int. J. Fertil. Womens Med.*, **43**, 56-64.

Matkovic, V., Fontana, D., Tominac, C., Goel, P. & Chesnut, C.H. III (1990) Factors that influence peak bone mass formation: a study of calcium balance and the inheritance of bone mass in adolescent females. *Am. J. Clin. Nutr.*, **52**, 878-888.

Mizuno, H., Hata, K., Kojima, K., Bonassar, L.J., Vacanti, C.A. & Ueda, M. (2006) A novel approach to regenerating periodontal tissue by grafting autologous cultured periosteum. *Tissue Eng.*, **12**, 1227-1335.

Myburgh, K.H., Bachrach, L.K., Lewis, B., Kent, K. & Marcus, R. (1993) Low bone mineral density at axial and appendicular sites in amenorrheic athletes. *Med. Sci. Sports Exerc.*, **25**, 1197-1202.

Myburgh, K.H., Hutchins, J., Fataar, A.B., Hough, S.F. & Noakes, T.D. (1990) Low bone density is an etiologic factor for stress fracture in athletes. *Ann. Intern. Med.*, **113**, 754-759.

Park, B.W., Hah, Y.S., Kim, D.R., Kim, J.R. & Byun, J.H. (2007) Osteogenic phenotypes and mineralization of cultured human periosteal-derived cells. *Arch. Oral Biol.*, **52**, 983-989.

Prior, J.C., Vigna, Y.M., Schechter, M.T. & Burgess, A.E. (1990) Spinal bone loss and ovulatory disturbances. *N. Engl. J. Med.*, **323**, 1221-1227.

Rozenberg, S., Vandromme, J., Ayata, N.B., Filippidis, M. & Kroll, M. (1999) Osteoporosis management. *Int. J. Fertil. Womens Med.*, **44**, 241-249.

Welten, D.C., Kemper, H.C.G., Post, G.B., Mechelen, W.V., Twisk, J., Lips, P. & Teule, G.J. (1994) Weight-bearing activity during youth is a more important factor for peak bone mass than calcium intake. *J. Bone Miner. Res.*, **9**, 1089-1096.

Yeh, J.K. & Aloia, J.F. (1990) Effects of physical activity on calciotropic hormones and calcium balance in rats. *Am. J. Physiol.*, **258**, E263-268.

Yeh, J.K., Aloia, J.F. & Yasumura, S. (1989) Effect of physical activity on calcium and phosphorus metabolism in the rat. *Am. J. Physiol.*, **256**, E1-6.

Yingling, V.R., Davies, S. & Silva, M.J. (2001) The effects of repetitive physiologic loading on bone turnover and mechanical properties in adult female and male rats. *Calcif. Tissue Int.*, **68**, 235-239.

SPINE Volume 34, Number 16, pp 1644–1649

Evidence of Enhanced Expression of Osteopontin in Spinal Hyperostosis of the Twy Mouse

Atsuomi Aiba, MD,*† Arata Nakajima, MD, PhD,*‡ Akihiko Okawa, MD, PhD,* Masao Koda, MD, PhD,*‡ and Masashi Yamazaki, MD, PhD*

Study Design. Gene expression and protein localization of osteopontin (OPN) in spinal hyperostosis of the twy mouse by means of in situ hybridization, immunohistochemistry, and Northern blot analysis.

Objective. To verify the involvement of OPN in spinal hyperostosis in the twy mouse and elucidate its ossification pattern at molecular levels.

Summary of Background Data. OPN is a molecule that consistently colocalizes with ectopic calcification in human pathologic conditions. The twy mouse, which shows ectopic calcification of the spinal ligament resulting in hind limb paralysis, is considered to be a model for human ossification of the posterior longitudinal ligament of the spine.

Methods. Twenty-eight each of age-matched twy, heterozygote, and wild-type mice were killed at 2, 4, 8, 12, and 16 weeks old and subject to histologic and/or molecular analyses. Sections were hybridized with RNA probes for OPN and also stained with anti-OPN antibodies. Total cellular RNA was extracted from the cervicothoracic spine of each genotype at 2- and 16-week-old, and gene expression for OPN and COL10A1 was quantified by Northern blot analysis.

Results. Enhanced expression of OPN mRNA was observed in spinal hyperostotic lesions of the twy mouse, specifically in cells of the spinal ligament and chondrogenic cells in the outer layer of the anulus fibrosus. These trends were also confirmed by immunohistochemical analyses. Northern blot analysis showed that a considerable amount of OPN transcripts was detected in all genotypes at 2 weeks old, but the robust expression of OPN mRNA was maintained only in twy mice at 16 weeks old. COL10A1 transcripts were hardly detected regardless of the genotype at 16 weeks old.

Conclusion. OPN was overexpressed in the hyperostotic spinal lesions of twy mice, and the hyperostosis was induced mainly by ectopic ossification of the spinal ligament. Because OPN is considered to be an inhibitor of calcification, further studies will be necessary to verify whether OPN overexpressed in the twy mouse is functional.

From the *Department of Orthopedic Surgery, Chiba University Graduate School of Medicine, Chiba, Japan; †Department of Orthopedic Surgery, Numazu Municipal Hospital, Numazu, Japan; and ‡Department of Orthopedic Surgery, Chiba Aoba Municipal Hospital, Chiba, Japan.
Acknowledgment date: November 13, 2008. Revision date: January 30, 2009. Acceptance date: February 10, 2009.
The legal regulatory status of the device(s)/drug(s) that is/are the subject of this manuscript is not applicable in my country.
Funds were received in support of this work. No benefits in any form have been or will be received from a commercial party related directly or indirectly to the subject of this manuscript.
Supported by a Grant-in-Aid for Scientific Research from the Ministry of Education, Science and Culture of Japan.
Address correspondence and reprint requests to Masashi Yamazaki, MD, PhD, Department of Orthopaedic Surgery, Chiba University Graduate School of Medicine, 1-8-1 Inohana, Chuo-ku, Chiba 260-8670, Japan; E-mail: masashiy@faculty.chiba-u.jp

Key words: osteopontin (OPN), ectopic calcification, spinal hyperostosis, twy mouse. **Spine 2009;34:1644–1649**

The twy (tiptoe-walking Yoshimura) mouse, established in Japan in 1978 by mating siblings of the ICR strain of mice, is a mutant (gene symbol: *ttw*) showing multiple osteochondral lesions.[1] We have used this mouse as a model for ossification of the posterior longitudinal ligament of the spine (OPLL), a disorder that causes severe cervical myelopathy in humans.[2–7] The incidence of OPLL is 1.5% among the Japanese population over 50 years old. Today, OPLL is known to occur worldwide, although it continues to occur particularly in Asia. Consequently, the hyperostotic changes in the cervical vertebral cortex of the twy mouse has drawn attention as a useful model for human ankylosing spinal hyperostosis[8] and/or diffuse idiopathic skeletal hyperostosis.[9] Both disease entities are thought to be quite similar to OPLL.

We previously determined that the twy phenotype is caused by a nonsense mutation (glycine 568 to stop) in the *Npps* gene, which encodes nucleotide pyrophosphatase.[2] This enzyme regulates soft tissue calcification and bone mineralization by producing inorganic pyrophosphatase, a major inhibitor of calcification.[10–13] Thus, the hyperostotic phenotype of the twy mouse is thought to result from dysfunction of nucleotide pyrophosphatase.

Osteopontin (OPN), a secreted glycosylated phosphoprotein, is one of the major noncollagenous proteins in bone matrix. It binds with high affinity to hydroxyapatite, possibly through its asparatic acid-rich region, and it may participate in physiologic tissue mineralization.[14] In addition, OPN interacts with the vitronectin receptor ($\alpha v\beta 3$ integrin) on osteoclasts through its Arg-Gly-Asp (RGD) sequence, implicating OPN as a potentially important participant in bone resorption.[14,15] OPN is also well known as a molecule that consistently colocalizes with ectopic calcification, and is an acidic phosphoprotein normally found in bone, teeth, kidney, and epithelial lining tissues. Expression of OPN mRNA is increased under conditions of injury and disease in many tissues, and it is closely associated with calcified deposits found in numerous pathologies including atherosclerotic lesions, aortic stenosis, kidney stones, and tumors.[16] Recent *in vitro* studies support a role for OPN as an inhibitor of calcification and hydroxyapatite growth.[17–19] Conversely, the colocalization of OPN with biomineralization in hard tissues and its ability to bind and poten-

tially orient calcium[20] suggest that OPN may promote ectopic calcification *in vivo*.

Although OPN is a key molecule involved in ectopic calcification associated with normal and/or pathologic conditions, there have been no reports showing association of OPN with spinal hyperostosis, which is the most characteristic phenotype of the twy mouse. To determine the involvement of OPN in ectopic calcification of the spinal ligament in this mutant, we assessed spatial and temporal gene expression for OPN in the spine and compared its expression profile among twy, heterozygote, and wild-type mice.

Materials and Methods

Animals and Tissue Preparation

The animals used in this study were 28 each of age-matched twy, heterozygote, and wild-type mice that have the ICR strain. At 2, 4, 8, 12, and 16 weeks old, mice were killed under anesthesia and their cervical spine was removed after perfusion-fixation with 4% paraformaldehyde in 0.1 M phosphate buffer. These experimental procedures were approved by the Animal Care and Use Committee of Chiba University, Japan.

Samples were then dehydrated and decalcified with 20% EDTA (pH: 7.4). After decalcification, the cervical spine was bisected sagittally in the median plane. Tissues were then embedded in paraffin and midsagittal 6-μm-thick sections were cut and mounted on silane-coated slides.

Preparation of Probes

The following cDNA clones were used as hybridization probes in this study: mouse pro-α1(X) collagen (COL10A1) cDNA containing a 0.60-kb fragment and mouse osteopontin cDNA containing a 1.2-kb fragment (a gift from Dr. S. Nomura, Osaka University, Japan). Specificity of these probes was confirmed previously.[21–24]

In Situ *Hybridization*

To compare distribution of cells expressing OPN mRNA in the cervical spine of twy and wild-type mice, sections were hybridized with probes for OPN. Digoxigenin-11-uridine 5-triphosphate-labeled single-strand RNA probes (antisense and sense probes) for mouse OPN cDNA (1.2-kb) were prepared. *In situ* hybridization was carried out as previously described.[21,22,24,25] Briefly, sections were hybridized with antisense probes at 50°C for 16 hours, and signals were detected using the digoxigenin detection kit (Roche Molecular Biochemicals, Indianapolis, IN). After signal detection, sections were counterstained with methyl-green. Sense probes were used to exclude the possibility of nonspecific signals.

Immunohistochemistry

To clarify the localization of OPN in the cervical spine of twy and wild-type mice, sections were reacted with antimouse OPN rabbit antibodies (1:100; LSL, Tokyo, Japan) as previously described.[26] Signals were detected using diaminobenzidine. Counterstaining was performed with Mayer's Hematoxyline. For negative-control sections, the same procedures were used but the primary antibody was replaced by nonimmune rabbit IgG (Vectastain, Vector Laboratories, Burlingame, CA).

RNA Extraction and Northern Blot Analysis

For RNA extraction, 4 mice of each genotype were killed as described earlier at 2- and 16-week-old, and the cervicothoracic spine was harvested. Tissues were frozen immediately in liquid nitrogen and stored at −80°C until RNA isolation was performed. Total cellular RNA was extracted using TRIzol (Gibco BRL, Rockville, MD) according to the manufacturer's instructions. Twenty μg of total RNA from each sample was subjected to 1% agarose gel electrophoresis and transferred to a nylon membrane (Hybond-XL; Amersham Pharmacia Biotech, Buckinghamshire, UK). cDNA probes were labeled with ^{32}P using a random priming method. Northern blot analysis was carried out as previously described.[21–24] The density of each band on the autoradiogram was estimated by an image analyzer (Image Gauge software, version 3.1; FUJIFILM, Tokyo, Japan).

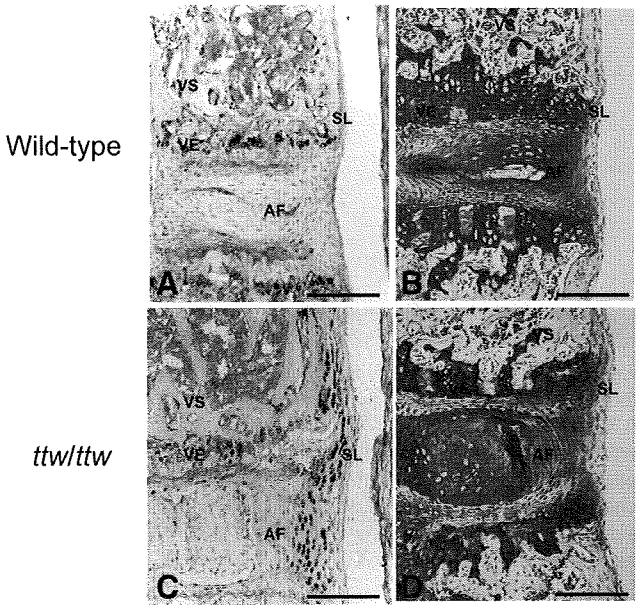

Figure 1. Expression of OPN mRNA in the cervical spine of wild-type and twy mice at 4 weeks old. In wild-type mice, expression of OPN mRNA was restricted to cells of the vertebral end plate and to osteoblasts of the vertebral primary spongiosa (**A**). In contrast, in twy mice (ttw/ttw), OPN mRNA was also detected in cells of the spinal ligament and cells of the outer layer of the anulus fibrosus (**C**). Cellular hypertrophy of these OPN mRNA-positive cells was more evident in twy mice than in the wild-type (**B, D**). VE indicates vertebral end plate; VS, vertebral primary spongiosa; SL, spinal ligament; and AF, anulus fibrosus. Scale bars = 200 μm.

Results

Analysis of OPN mRNA Expression by In Situ *Hybridization*

OPN mRNA was detected in cells of the vertebral end plate both in wild-type and twy mice from 2 weeks old, and there was no evident difference in its expression pattern between genotypes (data not shown).

At 4 weeks old, expression of OPN mRNA was restricted to cells in the vertebral end plate and osteoblasts in the vertebral primary spongiosa in wild-type mice (Figure 1A). In contrast, in twy mice, OPN was also detected in cells of the spinal ligament and cells in the outer layer of the anulus fibrosus (Figure 1C). Cellular hypertrophy of these OPN mRNA-positive cells was more evident in twy mice than in the wild-type (Figures 1B, D). The preferential expression of OPN in the spinal

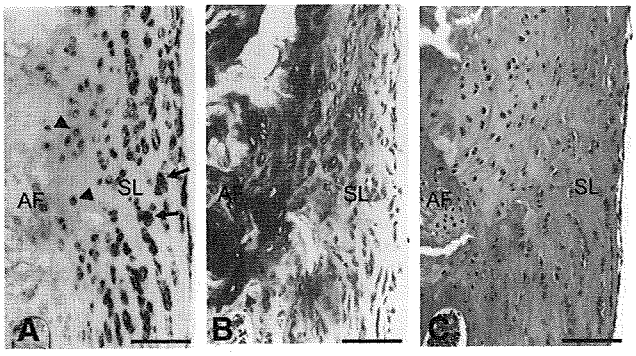

Figure 2. Expression of OPN mRNA in the posterior cervical spine of the twy mouse at 16 weeks old. Panels A to C are sequential sections. A strong OPN signal was detected in cells of the spinal ligament (**A**, arrows) and hypertrophic chondrocytes in the outer layer of the anulus fibrosus (**A**, arrowheads). The region containing OPN-positive chondrocytes in the anulus fibrosus showed metachromasia with TB staining (**B**). OPN-positive regions in the spinal ligament showed eosinophilia with HE staining (**C**). Scale bars = 50 μm.

ligament and anulus fibrosus in twy mice became more evident at 8- and 12-week-old (data not shown).

At 16 weeks old, the spinal ligament became hypertrophied in twy mice, and cells in both the posterior (Figure 2A, arrows) and anterior (Figure 4A, arrows) spinal ligaments expressed a strong signal for OPN mRNA. Hematoxyline and eosin (HE) staining revealed that these OPN-positive regions were histologically consistent with osteoid (Figure 2C). At this time point, some chondrogenic cells in the outer layer of the anulus fibrosus also expressed a strong signal for OPN mRNA (Figure 2A, arrowheads) and these regions showed metachromasia with toluidine-blue (TB) staining (Figure 2B). In contrast, the OPN signal was significantly diminished in age-matched wild-type mice (data not shown).

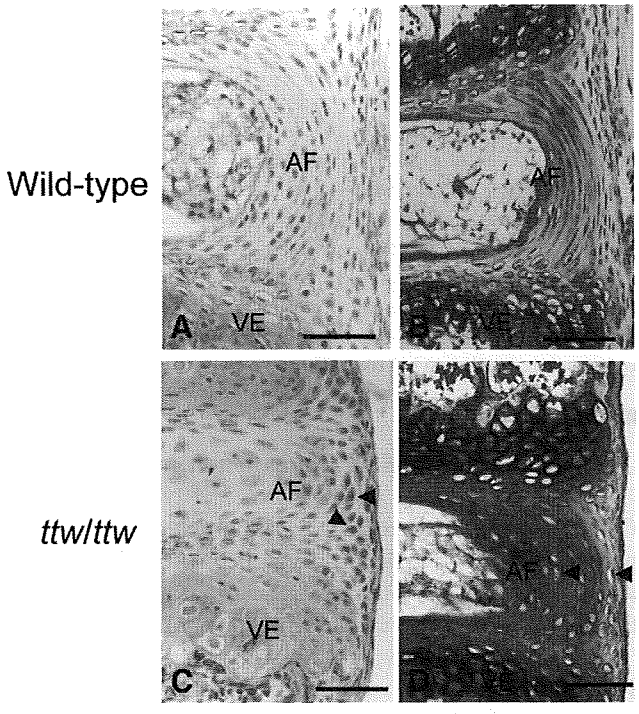

Figure 3. Localization of OPN protein in the cervical spine of wild-type and twy mice at 2 weeks old. In twy mice (ttw/ttw), OPN immunoreactivity was evident in cells of the outer layer of the anulus fibrosus. Most of the OPN-positive cells were hypertrophied and showed a round-shaped morphology (**C, D**, arrowheads). However, in wild-type mice, OPN immunoreactivity was weak and showed a spindle-shaped morphology (**A, B**). Scale bars = 50 μm.

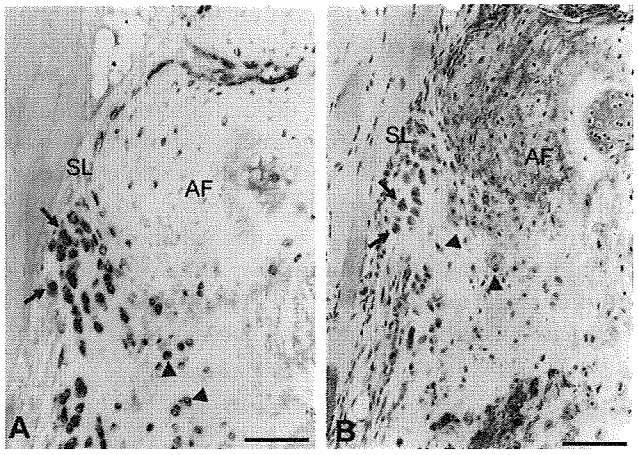

Figure 4. Expression of OPN mRNA (**A**) and localization of its protein (**B**) in the anterior cervical spine of the twy mouse at 16 weeks old. Panels A and B are sequential sections. A strong OPN mRNA signal was detected in cells of the spinal ligament (**A**, arrows) and chondrogenic cells in the outer layer of the anulus fibrosus (**A**, arrowheads). Localization of OPN protein was evident in cells that were also positive for OPN mRNA (**B**, arrows and arrowheads). Scale bars = 50 μm.

Analysis of OPN by Immunohistochemistry

At 2 weeks old, OPN immunoreactivity was detected in cells of the vertebral end plate both in wild-type and twy mice (data not shown). In addition, in twy mice, OPN was evident in cells in the outer layer of the anulus fibrosus. Most of the OPN-positive cells were hypertrophied and showed a round-shaped morphology (Figures 4C, D, arrowheads). However, in wild-type mice, OPN immunoreactivity was weak and showed a spindle-shaped morphology (Figures 4A, B).

From 4 weeks old on, in twy mice, OPN immunoreactivity was detected in cells in the spinal ligament (Figure 3B, arrows) and chondrogenic cells in the outer layer of the anulus fibrosus (Figure 3B, arrowheads), which was consistent with the expression pattern of OPN mRNA by *in situ* hybridization analysis. These trends were also seen in wild-type mice; however, OPN immunoreactivity was weak compared with that of twy mice (data not shown).

Analysis of OPN and COL10A1 mRNA by Northern Blot

At 2 week's old, considerable amounts of OPN transcripts were detected in all genotypes and there was no significant difference in the expression level among genotypes. At 16 weeks, robust expression of OPN mRNA was still detected in twy mice; however, it was reduced in the heterozygote and further reduced in wild-type mice (Figure 5).

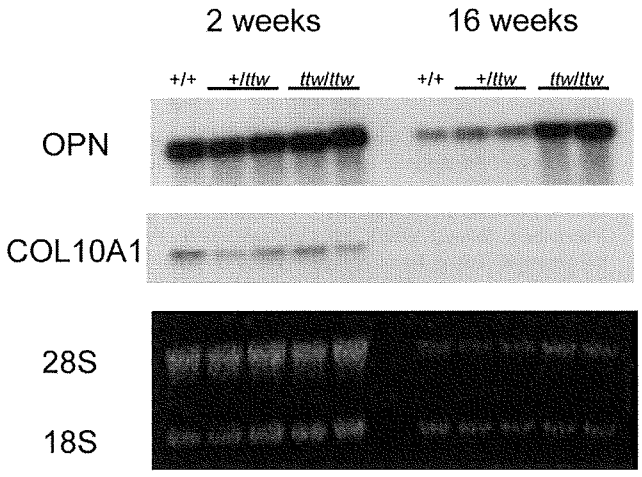

Figure 5. Temporal expression of OPN and COL10A1 mRNA in the cervicothoracic spine of wild-type, heterozygote (+/*ttw*), and twy mice (*ttw/ttw*) during growth. Twenty μg of total RNA from each sample was analyzed to quantify the levels of OPN and COL10A1 transcripts. At 2 weeks old, considerable amounts of OPN transcripts were detected in all genotypes with no significant difference in expression levels among them, while small amounts of COL10A1 transcripts were seen in all genotypes. At 16 weeks old, robust expression of OPN mRNA was still detected in twy mice, but no longer detected in the heterozygote or wild-type mice. Note that COL10A1 transcripts were hardly detected regardless of the genotype. Eighteen S and 28S served an internal standard for the amount and integrity of RNA preparation. Representative autographic images are shown.

To determine the ossification pattern for the spinal ligament of twy mice, we also investigated the temporal expression of the COL10A1 gene, an established marker for chondrocyte hypertrophy, during growth. At 2 weeks old, a small amount of COL10A1 transcripts was detected in all genotypes, with no significant differences noted among genotypes. Strikingly, at 16 weeks old, COL10A1 transcripts were hardly detected regardless of the genotype (Figure 5).

■ Discussion

The spinal lesion of the twy mouse is characterized by ectopic calcification that occurs in the outer layer of the anulus fibrosus from 4 weeks old and bony bridging over vertebral bodies that begins at 11 weeks old.[4] Histologic analyses using nondecalcified spinal tissues of twy mice showed intramembranous bone formation at the enthesis of the spinal ligament.[4,6] However, the present study using decalcified tissues demonstrated endochondral bone formation at the enthesis. Thus, ossification patterns for the spinal ligament of the twy mouse have been unknown to date.

In the spine of the twy mouse, OPN was detected in hypertrophic chondrocytes of the vertebral end plate, cells in the outer layer of the anulus fibrosus, cells in the spinal ligament, and osteoblasts in the primary spongiosa of the vertebral body. Of interest, from 4 weeks old on, expression of OPN in the twy mouse was enhanced in chondrogenic cells in the outer layer of the anulus fibrosus and cells in the spinal ligament, compared with age-matched wild-type mice. In particular, extracellular matrix around cells in the outer layer of the anulus fibrosus showed metachromasia with TB staining, suggesting that those cells possessed a chondrogenic phenotype. Furthermore, regions adjacent to the TB-stained area showed eosinophilia with HE staining, indicating that osteoid, immature bone is also formed there. Considering our previous study demonstrating localization of type II, IV, and XI collagen in the outer layer of the anulus fibrosus,[7] ossification of the spinal ligament in the twy mouse might be induced, at least in part, by endochondral ossification.

To determine whether ossification of the spinal ligament is mediated by endochondral bone formation, we extracted total RNA from the spine and investigated mRNA expression for OPN and COL10A1 at 2- and 16-week-old. During endochondral ossification, COL10A1 and OPN are expressed in hypertrophic chondrocytes. Although COL10A1 is specifically expressed in cells of chondrogenic lineage, OPN is expressed in cells of both chondrogenic and osteoblastic lineages.[21,22,24] At 2 weeks old, an equivalent amount of COL10A1 transcripts was detected in all genotypes. However, at 16 weeks old, COL10A1 transcripts were hardly detected regardless of genotype despite elevated levels of OPN seen in the twy mouse. These suggest that the major ossification process for the spinal ligament of twy mice is not canonical endochondral bone formation. At this point, in twy mice, a considerable amount of OPN was expressed in fibroblastic cells in hypertrophied spinal ligament rather than in hypertrophic chondrocytes in the anulus fibrosus. This also suggests that spinal hyperostosis of the twy mouse develops largely by ectopic ossification of the spinal ligament, but does not involve chondrocytes of vertebral disc-mediated endochondral ossification.

OPN, an extracellular matrix protein known to be important in cellular attachment, is also a useful marker for calcification during both intramembranous and endochondral ossification.[22–24] During fracture healing, expression of OPN is detected in osteocytes and osteoprogenitor cells in the subperiosteal callus,[27] but little OPN signal is seen in cuboidal osteoblasts.[25,27] Furthermore, OPN is preferentially expressed in late hypertrophic chondrocytes, but not in proliferating chondrocytes, and early hypertrophic chondrocytes in cartilaginous calluses.[22,24] Although OPN function in bone and cartilage metabolism remains to be elucidated, these observations suggest that OPN functions as a marker for calcification *in vivo*.

Overexpression of OPN in the spinal hyperostosis of the twy mouse seems understandable from the view point that OPN is a marker for calcification *in vivo*. Indeed, there have been many reports that OPN mRNA was overexpressed in pathologic lesions associated with ectopic calcification,[28–31] indicating that OPN may have a positive role in promoting calcification *in vivo*. OPN possesses the ability to bind significant amounts of Ca^{2+} through its electronegative glutamic and aspartic acid residues, serine/threonine kinase substrate sites, and putative calcium-binding mo-

tifs.[32] These properties of OPN likely contribute to ectopic calcification. However, the contribution of enhanced OPN expression to spinal hyperostosis seems to be paradoxical from the view point that OPN is an inhibitor of calcification. Why is spinal hyperostosis developed in the twy mouse despite local overexpression of OPN?

Previous *in vitro* and *in vivo* studies suggest that OPN not only inhibits mineral deposition, but also actively promotes its dissolution by physically blocking hydroxyapatite crystal growth and inducing expression of carbonic anhydrase II in monocytic cells, which promotes acidification of the extracellular milieu.[29] These findings indicate that recruitment of macrophages and/or monocytic cells and their bone-resorbing functions are important for OPN to regulate ectopic calcification. In other words, under abnormal ectopic ossification associated with overexpression of OPN, it should be considered that there might be some problems in OPN function.

Recently, it has emerged that OPN-knock-out mice are susceptible to ectopic calcification *in vivo*,[29,31] indicating that physiologic concentrations of OPN inhibit calcification. To the best of our knowledge, however, there have been no studies demonstrating the effects of an excessive amount of OPN on ectopic calcification *in vivo*. To explain spinal hyperostosis in the twy mouse associated with local overexpression of OPN, we think the possibility that overexpressed OPN in the spinal ligament does not fully exert its primary function as an inhibitor of calcification. Because it has been reported that phosphorylation of OPN is crucial for its anticarcific effects,[17,19,31] further studies will be necessary to verify whether OPN overexpressed in the twy mouse is functional (*i.e.*, phosphorylated).

In conclusion, the results presented here clearly establish overexpression of OPN in spinal hyperostosis of the twy mouse, and this hyperostosis was induced by ectopic ossification of the spinal ligament. Targeting OPN as a prime candidate molecule for inhibition of ectopic calcification may provide new therapeutic clues for hyperostotic diseases of the spine.

■ Key Points

- To verify the involvement of OPN in spinal hyperostosis in the twy mouse, a model for human OPLL, gene expression, and protein localization of OPN was analyzed by means of *in situ* hybridization, immunohistochemistry, and Northern blot analysis.
- OPN was overexpressed in hyperostotic spinal lesions of the twy mouse, and the hyperostosis was induced mainly by ectopic ossification of the spinal ligament.
- Because OPN is considered to be an inhibitor of calcification, further studies will be necessary to verify whether OPN overexpressed in the twy mouse is functional.

References

1. Hosoda Y, Yoshimura Y, Higaki S. Anew breed of mouse showing multiple osteochondral lesions: twy mouse [in Japanese]. *Ryumachi* 1981;21(suppl): 157–64.
2. Okawa A, Nakamura I, Goto S, et al. Mutation in *Npps* in a mouse model of ossification of the posterior longitudinal ligament of the spine. *Nat Genet* 1998;19:271–3.
3. Goto S, Yamazaki M. Pathogenesis of ossification of the spinal ligaments. In: Yonenobu K, Sakou T, Ono K, eds. *Ossification of the Posterior Longitudinal Ligament*. Tokyo, Japan: Springer-Verlag; 1997:29–37.
4. Tannno T. Experimental study on the spinal lesions in hyperostotic mouse (twy/twy): special reference to the pathogenesis of the spinal ligaments and to the action of ethane-1, 1-diphosphonate (EHDP) [in Japanese]. *J Jpn Orthop Assoc* 1992;66:1073–82.
5. Okawa A, Goto S, Moriya H. Calcitonin simultaneously regulates both periosteal hyperostosis and trabecular osteopenia in the spinal hyperostotic mouse (twy/twy) in vivo. *Calcif Tissue Int* 1999;64:239–47.
6. Terakado A, Tagawa M, Goto S, et al. Elevation of alkaline phosphatase activity induced by parathyroid hormone in osteoblast-like cells from the spinal hyperostotic mouse TWY (twy/twy). *Calcif Tissue Int* 1995;56:135–9.
7. Yamazaki M, Moriya H, Goto S, et al. Increased type IX collagen expression in the spinal hyperostotic mouse (twy/twy). *Calcif Tissue Int* 1991;48:182–9.
8. Forestier J, Lagier R. Ankylosing hyperostosis of the spine. *Clin Orthop* 1971;74:65–83.
9. Resnick D, Shaul SR, Robins JM. Diffuse idiopathic skeletal hyperostosis (DISH): Forestier's disease with extraspinal manifestations. *Radiology* 1975; 115:513–24.
10. Caswell AM, Ali SY, Russell RG. Nucleotide triphosphate pyrophosphatase of rabbit matrix vesicles, a mechanism for the generation of inorganic pyrophosphate in epiphyseal cartilage. *Biochim Biophys Acta* 1987;924:276–83.
11. Caswell AM, Russell RG. Evidence that ecto-nucleoside-triphosphate pyrophosphatase serves in the generation of extracellular inorganic pyrophosphate in human bone and articular cartilage. *Biochim Biophys Acta* 1988; 966:310–7.
12. Huang R. Expression of the murine plasma cell nucleotide pyrophosphohydrolase PC-1 is shared by human liver, bone, and cartilage cells: regulation of PC-1 expression in osteosarcoma cells by transforming growth factor-beta. *J Clin Invest* 1994;94:560–7.
13. Fleisch H. Diphosphonates: history and mechanisms of action. *Metab Bone Dis Relat Res* 1981;3:279–88.
14. Oldberg A, Franzen A, Heinegard D. Cloning and sequence analysis of rat bone sialoprotein (osteopontin) cDNA reveals an Arg-Gly-Asp cell-binding sequence. *Proc Natl Acad Sci USA* 1986;83:8819–23.
15. Miyauchi A, Alvarez J, Greenfield EM. Recognition of osteopontin and related peptides by an (alpha v beta 3) integrin stimulates immediate cells signals in osteoclasts. *J Biol Chem* 1991;266:20369–74.
16. Giachelli CM, Schwartz SM, Liaw L. Molecular and cellular biology of osteopontin. *Trends Cardiovasc Med* 1995;5:88–95.
17. Hunter GK, Kyle CL, Goldberg HA. Modulation of crystal formation by bone phosphoproteins: structural specificity of the osteopontin-mediated inhibition of hydroxyapatite formation. *Biochem J* 1994;300:723–8.
18. Boskey AL, Maresca M, Ullrich W, et al. Osteopontin-hydroxyapatite interactions in vitro: inhibition of hydroxyapatite formation and growth in a gelatin-gel. *Bone Miner* 1993;22:147–59.
19. Jono S, Peinado C, Giachelli CM. Phosphorylation of osteopontin is required for inhibition of vascular smooth muscle cell calcification. *J Biol Chem* 2000; 275:20197–203.
20. Groski JP. Acidic phosphoproteins from bone matrix: a structural rationalization of their role in biomineralization. *Calcif Tissue Int* 1992;50:391–6.
21. Nakajima F, Ogasawara A, Goto K, et al. Spatial and temporal gene expression in chondrogenesis during fracture healing and the effects of basic fibroblast growth factor. *J Orthop Res* 2001;19:935–44.
22. Nakazawa T, Nakajima A, Shiomi K, et al. Effects of low-dose, intermittent treatment with recombinant human parathyroid hormone (1–34) on chondrogenesis in a model of experimental fracture healing. *Bone* 2005; 37:711–9.
23. Nakajima F, Nakajima A, Ogasawara A, et al. Effects of a single percutaneous injection of basic fibroblast growth factor on the healing of a closed femoral shaft fracture in the rat. *Calcif Tissue Int* 2007;81:132–8.
24. Ogasawara A, Nakajima A, Nakajima F, et al. Molecular basis for affected cartilage formation and bone union in fracture healing of the streptozotocin-induced diabetic rat. *Bone* 2008;43:832–9.
25. Yamazaki M, Majeska RJ, Yoshioka H, et al. Spatial and temporal expression of fibril-forming minor collagen genes (Type V and XI) during fracture healing. *J Orthop Res* 1997;15:757–64.

26. Hashimoto M, Koda M, Ino H, et al. Upregulation of osteopontin in rat spinal cord microglia after traumatic injury. *J Neurotrauma* 2003;20:287–96.
27. Hirakawa K, Hirota S, Ikeda T, et al. Localization of the mRNA for bone matrix proteins during fracture healing as determined by in situ hybridization. *J Bone Miner Res* 1994;9:1551–7.
28. Ikeda T, Shirasawa T, Esaki Y, et al. Osteopontin mRNA is expressed by smooth muscle-derived form cells in human atherosclerotic lesions of the aorta. *J Clin Invest* 1993;92:2814–20.
29. Steitz SA, Speer MY, McKee MD, et al. Osteopontin inhibits mineral deposition and promotes regression of ectopic calcification. *Am J Pathol* 2002;161:2035–46.
30. Harmey D, Hessle L, Narisawa S, et al. Concerted regulation of inorganic pyrophosphate and osteopontin by Akp2, Enpp1, and Ank: an integrated model of the pathogenesis of mineralization disorders. *Am J Pathol* 2004; 164:1199–209.
31. Ohri R, Tung E, Rajachar R, et al. Mitigation of ectopic calcification in osteopontin-deficient mice by exogenous osteopontin. *Calcif Tissue Int* 2005;76:307–15.
32. Chen Y, Bal BS, Groski JP. Calcium and collagen binding properties of osteopontin, bone sialoprotein, and bone acidic glycoprotein-75 from bone. *J Biol Chem* 1992;276:24871–8.

Journal of Clinical Neuroscience 17 (2010) 320–324

Contents lists available at ScienceDirect

Journal of Clinical Neuroscience

journal homepage: www.elsevier.com/locate/jocn

Clinical Study

Static versus dynamic factors for the development of myelopathy in patients with cervical ossification of the posterior longitudinal ligament

Takayuki Fujiyoshi, Masashi Yamazaki *, Akihiko Okawa, Junko Kawabe, Koichi Hayashi, Tomonori Endo, Takeo Furuya, Masao Koda, Kazuhisa Takahashi

Spine Section, Department of Orthopaedic Surgery, Chiba University Graduate School of Medicine, 1-8-1 Inohana, Chuo-ku, Chiba 260-8677, Japan

ARTICLE INFO

Article history:
Received 20 April 2009
Accepted 29 June 2009

Keywords:
Cervical myelopathy
Dynamic factor
Laminoplasty
Ossification of posterior longitudinal ligament
Static factor

ABSTRACT

We studied 27 patients with cervical ossification of the posterior longitudinal ligament (OPLL) but no clinical symptoms of myelopathy. We investigated the occupation ratio of the spinal canal by OPLL with cervical radiographs, assessed the morphological types of OPLL, and measured the segmental range of motion (ROM) at the level of maximum cord compression on flexion and extension radiographs. Patients were classified as having continuous-type OPLL (17 patients), mixed-type OPLL (seven patients), or segmental-type OPLL (three patients). The segmental ROM was negatively correlated with the OPLL occupation ratio ($r = -0.49$, $p < 0.01$). No patient developed myelopathy during the study period. Three patients with massive OPLL did not develop myelopathy and the mobility of their cervical spine was highly restricted, suggesting that dynamic factors such as the segmental ROM preferentially contribute to the development of myelopathy in patients with cervical OPLL. Thus, by controlling the dynamic factors (hypermobility), we might be able to reduce neurological deterioration in patients with cervical OPLL.

1. Introduction

Ossification of the posterior longitudinal ligament (OPLL) of the cervical spine results in static compression of the spinal cord that causes myelopathy.[1–3] Both anterior and posterior surgical approaches have been performed for cervical myelopathy due to OPLL,[1,2,4,5] and several studies have shown that the anterior surgical approach results in a better surgical outcome when the occupation ratio by OPLL is large,[2,4] indicating that complete removal of the static compression factor is important in the treatment of myelopathy.

Dynamic factors, such as the mobility of the spinal column, are also important in the development of myelopathy when a considerable degree of the canal is occupied by OPLL.[6–8] However, the contribution of dynamic factors to the development of myelopathy in cervical OPLL patients has not been fully determined. In the present study, we radiographically and clinically evaluated patients who had cervical OPLL but no symptoms of myelopathy, and analyzed the contribution of static and dynamic factors to the development of myelopathy.

2. Materials and methods

From April 2000 through March 2007, 27 patients with cervical OPLL (11 men, 16 women, mean age at first diagnosis 63.3 years [range, 37–78 years]) in whom the space available for the spinal cord (SAC) (Fig. 1A) at the cervical spine was $\leqslant 12$ mm visited our institute for initial consultation. When the patients were diagnosed with cervical OPLL, they had no clinical symptom of myelopathy. The mean follow-up period for all the patients was 59 months (range, 12–95 months).

Using cervical radiographs, we measured the occupation ratio of the spinal canal by OPLL [(thickness of OPLL/anteroposterior diameter of the bony spinal canal) × 100][8] (Fig. 1A). Morphologically, patients were classified as continuous, mixed, segmental, or localized OPLL types according to the criteria of the Japanese Investigation Committee on the Ossification of the Spinal Ligaments.[9] We also evaluated the segmental range of motion (ROM) at the maximum cord compression level based on flexion and extension radiographs[8] (Fig. 1B), and on T2-weighted MRI we examined the high signal change in the spinal cord. The patients' clinical course was assessed using the Japanese Orthopaedic Association (JOA) scoring system for cervical myelopathy.[8] On physical examination, we assessed the patients' deep tendon reflexes of the lower extremities and the Babinski reflex.

For statistical analysis we applied the Fisher's exact probability test and Pearson's correlation test. A $p < 0.05$ was considered sig-

* Corresponding author. Tel.: +81 43 226 2117; fax: +81 43 226 2116.
E-mail address: masashiy@faculty.chiba-u.jp (M. Yamazaki).

0967-5868/$ - see front matter © 2009 Elsevier Ltd. All rights reserved.
doi:10.1016/j.jocn.2009.06.023

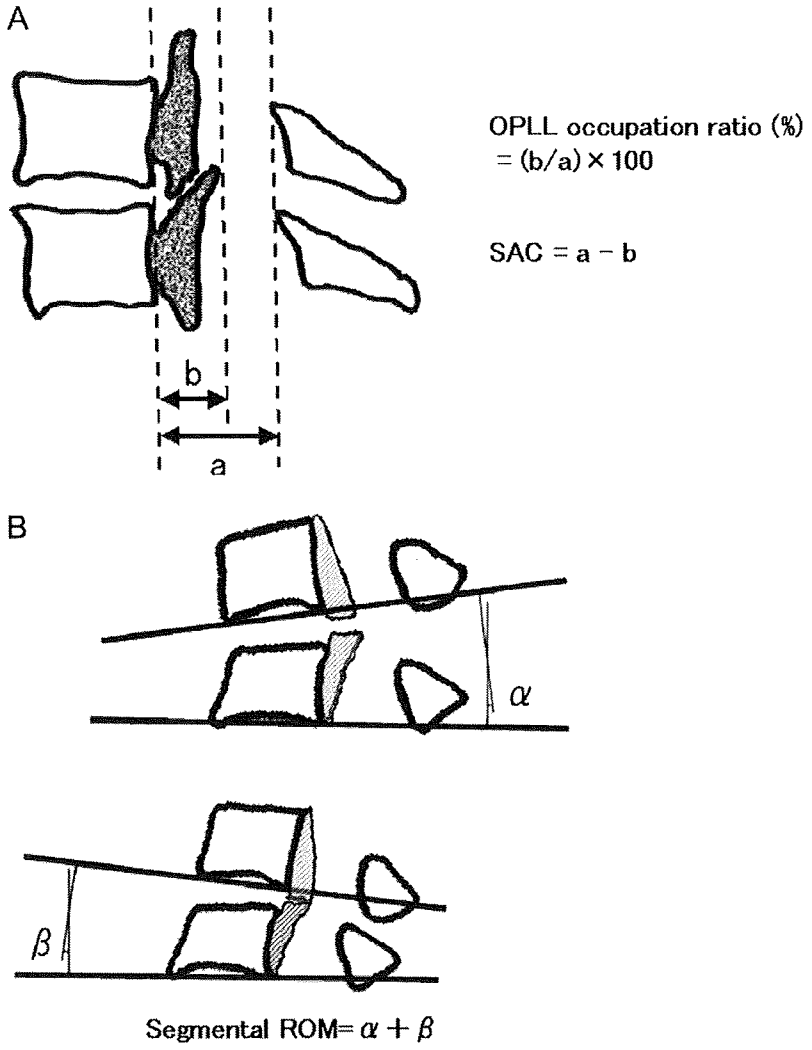

Fig. 1. Schematics showing the radiographic parameters assessed. (A) The ossification of the posterior longitudinal ligament (OPLL) occupation ratio and space available for the spinal cord (SAC) were measured from lateral cervical radiographs. (B) The segmental range of motion (ROM) at the maximum cord compression level was measured from flexion and extension radiographs.

Table 1
Radiographic findings for 27 patients with ossification of the posterior longitudinal ligament

	Type of OPLL[†]		
	Continuous	Mixed	Segmental
No. patients (*n*)	17[a]	7	3
SAC (mm)	7.6 ± 2.3 (3–12)	7.8 ± 1.0 (7–9)	9.4 ± 2.8 (7–12)
Occupation ratio (%)	42.5 ± 11.1 (25–64)	39.4 ± 7.6 (29–50)	27.7 ± 3.3 (25–31)
Segmental ROM (°)	2.4 ± 3.0 (0–9)	4.9 ± 2.9 (1–10)	9.7 ± 4.5 (5–14)

OPLL = ossification of the posterior longitudinal ligament, occupation ratio = occupation ratio of spinal canal by OPLL, ROM = range of motion (intervertebral disc mobility at the maximum cord compression level), SAC = space available for the spinal cord (see Fig. 1).
[†] Mean ± standard deviation (range).
[a] Statistically different from mixed-type OPLL and segmental-type OPLL ($p < 0.05$).

nificant. Data are presented as the mean ± standard deviation of the mean.

3. Results

3.1. Radiographic findings

Of the 27 patients analyzed, 17 (63%) were classified with the continuous type, 7 (26%) with the mixed type, and 3 (11%) with the segmental type of OPLL (Table 1), and the incidence of patients with continuous-type OPLL was significantly higher than that for the other types ($p < 0.05$).

The mean OPLL occupation ratio was 39.8% for all types. It was 42.5% in patients with continuous-type OPLL, 39.4% in patients with mixed-type OPLL, and 27.7% in patients with segmental-type OPLL (Table 1). The mean segmental ROM at the level of maximum cord compression was 3.8 degrees. It was 2.4 degrees in patients with continuous-type OPLL, 4.9 degrees in patients with

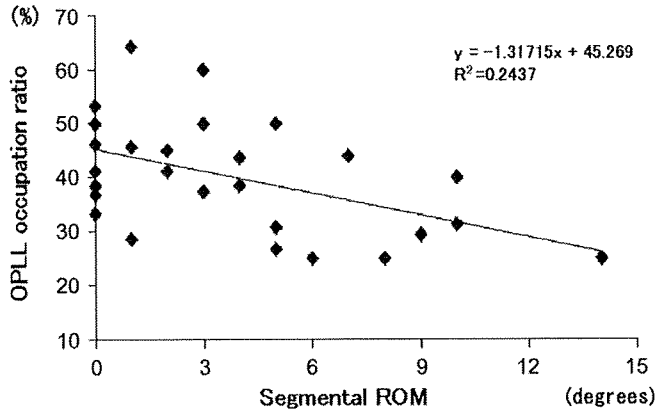

Fig. 2. The relationship between the ossification of the posterior longitudinal ligament (OPLL) occupation ratio and the segmental range of motion (ROM) in the cervical spine of 27 patients showing that as OPLL occupation ratio increased, the ROM decreased ($y = -131715x + 45.269$ [$r = -0.49$; $p < 0.01$]).

Table 2
Characteristics of three patients with an ossification of the posterior longitudinal ligament occupation ratio greater than 50%

	Patient 1	Patient 2	Patient 3
Age (yrs)/Gender	65/F	37/F	67/M
Sites of OPLL	C2-C5	C2-C7	C4-C6
Maximum cord compression level	C4-C5	C5-C6	C4-C5
Type of OPLL	Continuous	Continuous	Continuous
Occupation ratio (%)	64	60	53
SAC (mm)	3	3	6
Segmental ROM (degrees)	1	3	0
T2-high signal change	None	None	None
Deep tendon reflexes	Hyper	Hyper	Normal
Babinski reflex	+	+	+

OPLL = ossification of the posterior longitudinal ligament, occupation ratio = occupation ratio of spinal canal by OPLL, ROM = range of motion (intervertebral disc mobility at the maximum cord compression level), SAC = space available for the spinal cord, T2-high signal change = high signal change in T2-weighted MRI, yrs = years, Hyper = hyperactive (See Fig. 1).

mixed-type OPLL, and 9.7 degrees in a patient with segmental-type OPLL (Table 1). A significant negative correlation was detected between the segmental ROM and the OPLL occupation ratio by Pearson's correlation test ($r = -0.49$, $p < 0.01$) (Fig. 2). Three patients had an OPLL occupation ratio >50% and a SAC of ⩽6 mm (Table 2). All three patients had continuous-type OPLL, and their segmental ROM ranged from 0 degrees to 3 degrees.

Using T2-weighted MRI, we were able to analyze the signal intensity of the spinal cord at the maximum compression level in 18 of the 27 patients. None of the patients showed high signal change in the spinal cord.

3.2. Clinical findings

At first diagnosis, none of the 27 patients showed any motor, sensory, or bladder dysfunction, and their JOA scores were 17 points (full score). Regarding their physical examination, the deep tendon reflexes of the lower extremities were hyperactive in 10 of 27 patients (37%) and the Babinski reflex was positive in 6 of 27 patients (22%). During follow-up, none of the patients developed myelopathy, and the incidence of hyperactive deep tendon reflex and Babinski reflex remained unchanged.

3.3. Illustrative patient

3.3.1. Patient 1 (OPLL occupation ratio >50%)

A 65-year-old woman was diagnosed with continuous-type OPLL from C2 to C5, and the maximum cord compression was at C4/5. Her OPLL occupation ratio was 64% and the SAC was 3 mm. The patient's segmental ROM was 1 degree at the C4/5 level (Fig. 3A, B), indicating that she had massive OPLL, but no segmental hypermobility. Her deep tendon reflexes of the lower extremities were hyperactive, and her Babinski reflex was positive. T2-weighted MRI showed anterior compression of the spinal cord from C3/4 to 4/5, but no high signal change in the spinal cord (Fig. 3C, D). In spite of massive OPLL, the patient did not develop myelopathy, possibly due to the lack of dynamic factors (no hypermobility) at the level of cord compression.

4. Discussion

Static compression factors are important in the development of myelopathy in cervical OPLL patients, including the occupation ratio of the spinal canal by OPLL and the residual space available for the spinal cord.[2,4] Iwasaki et al. reported that the surgical outcome after laminoplasty was insufficient in patients with an OPLL occupation ratio >60% and hill-shaped ossification.[1] Tani et al. reported that anterior decompression surgery was superior to laminoplasty in cervical OPLL patients when their occupation ratio was more than 50%.[4]

Recent reports have described the importance of dynamic factors, including mobility of the spinal column, in the development of myelopathy in patients who have a considerable degree of canal occupation by OPLL.[7,8,10] Matsunaga et al. analyzed 247 patients with cervical OPLL, and reported that when the SAC was <6 mm, all patients developed myelopathy, but when the SAC was >14 mm, no patients developed myelopathy. This indicates that the static compression factor preferentially contributed to the development of myelopathy. However, they also reported that when the SAC was between 6 mm and 14 mm, patients with a larger C1–C7 ROM preferentially developed myelopathy, indicating that this dynamic factor also contributed to the development of myelopathy.[7] Ogawa et al. analyzed long-term results after laminoplasty for cervical OPLL patients, and reported that patients with segmental type OPLL and a larger C2–C7 ROM had poor surgical outcomes.[10] We also previously reported that a larger segmental ROM at the level of maximum cord compression was a risk factor leading to poor surgical outcome after laminoplasty for cervical OPLL patients.[8]

In the present study, we characterized patients who had cervical OPLL but no clinical symptoms of myelopathy. The results demonstrated that even in patients with massive OPLL, myelopathy may not develop when the mobility of the cervical spine is highly restricted. We paid particular attention to three patients who had OPLL occupation ratios of more than 50% (Table 2). In spite of the remarkable static compression in these patients, myelopathy did not develop, possibly because the mobility of their cervical spine was highly restricted. These findings suggest that segmental ROM (a dynamic factor) at the level of maximum cord compression preferentially contributes to the development of myelopathy rather than static compression factors. We speculate that if we control this dynamic factor, we will be able to reduce neurological deterioration in cervical OPLL patients.

Our findings highlight that when performing surgery on cervical OPLL patients with canal stenosis we should consider not only the need for decompression of the spinal cord but also the suppression of dynamic factors. We believe that complete excision of the ossified mass using an anterior approach together with stabilization of the spinal column by a strut bone graft is theoretically the best

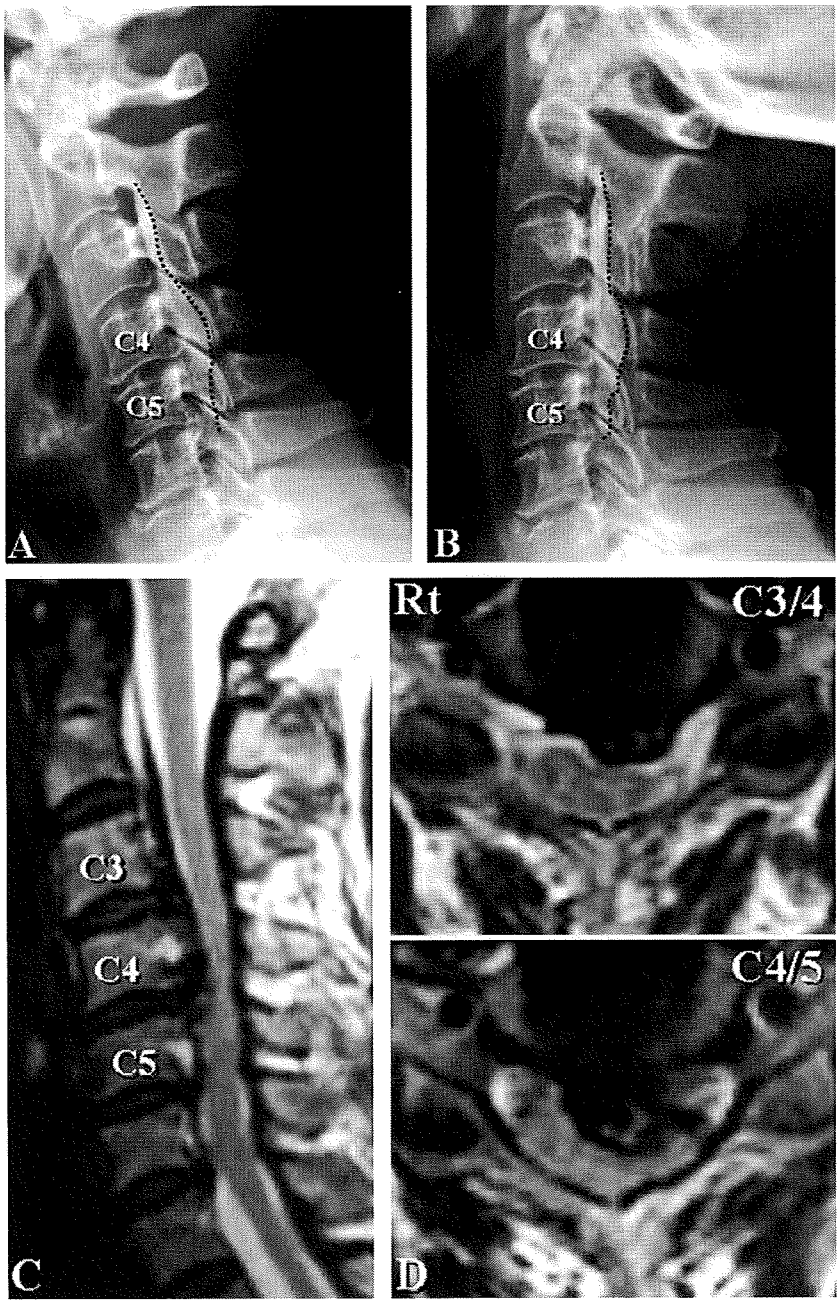

Fig. 3. (A) Flexion and (B) extension cervical radiographs at the initial visit of a 65-year-old woman with continuous type ossification of the posterior longitudinal ligament (OPLL) (patient 1) showing that the segmental range of motion was 1 degree at C4/5. T2-weighted (C) mid-sagittal and (D) axial MRI indicated anterior compression of the spinal cord at multiple levels, but high signal change was not apparent.

procedure. However, in spite of the superiority of anterior surgery, some patients, especially older patients, do not choose anterior surgery because the postoperative course is difficult to tolerate. Based on the present findings, when laminoplasty is selected for such patients, the addition of posterior instrumented fusion is desirable for stabilizing the spine and decreasing damage to the spinal cord.

Acknowledgement

This work was supported by the Health Labour Science Research Grant of Japan.

References

1. Iwasaki M, Okuda S, Miyauchi A, et al. Surgical strategy for cervical myelopathy due to ossification of the posterior longitudinal ligament: Part 1: clinical results and limitations of laminoplasty. *Spine* 2007;**32**:647–53.
2. Iwasaki M, Okuda S, Miyauchi A, et al. Surgical strategy for cervical myelopathy due to ossification of the posterior longitudinal ligament: Part 2: advantages of anterior decompression and fusion over laminoplasty. *Spine* 2007;**32**:654–60.
3. Ono K, Ota H, Tada K, et al. Ossified posterior longitudinal ligament: a clinicopathological study. *Spine* 1997;**2**:126–38.
4. Tani T, Ushida T, Ishida K, et al. Relative safety of anterior microsurgical decompression versus laminoplasty for cervical myelopathy with a massive ossified posterior longitudinal ligament. *Spine* 2002;**27**:2491–8.
5. Matsuoka T, Yamaura I, Kurosa Y, et al. Long-term results of the anterior floating method for cervical myelopathy caused by ossification of the posterior longitudinal ligament. *Spine* 2001;**26**:241–8.

6. Matsunaga S, Sakou T, Hayashi K, et al. Trauma-induced myelopathy in patients with ossification of the posterior longitudinal ligament. *J Neurosurg* 2002;**97**:172–5.
7. Matsunaga S, Kukita M, Hayashi K, et al. Pathogenesis of myelopathy in patients with ossification of the posterior longitudinal ligament. *J Neurosurg* 2002;**96**:168–72.
8. Masaki Y, Yamazaki M, Okawa A, et al. An analysis of factors causing poor surgical outcome in patients with cervical myelopathy due to ossification of the posterior longitudinal ligament: anterior decompression with spinal fusion versus laminoplasty. *J Spinal Disord Tech* 2007;**20**:7–13.
9. Tsuyama N. Ossification of the posterior longitudinal ligament of the spine. *Clin Orthop Relat Res* 1984;**184**:71–84.
10. Ogawa Y, Chiba K, Matsumoto M, et al. Long-term results after expansive open-door laminoplasty for the segmental-type of ossification of the posterior longitudinal ligament of the cervical spine: a comparison with nonsegmental-type lesions. *J Neurosurg Spine* 2005;**3**:198–204.

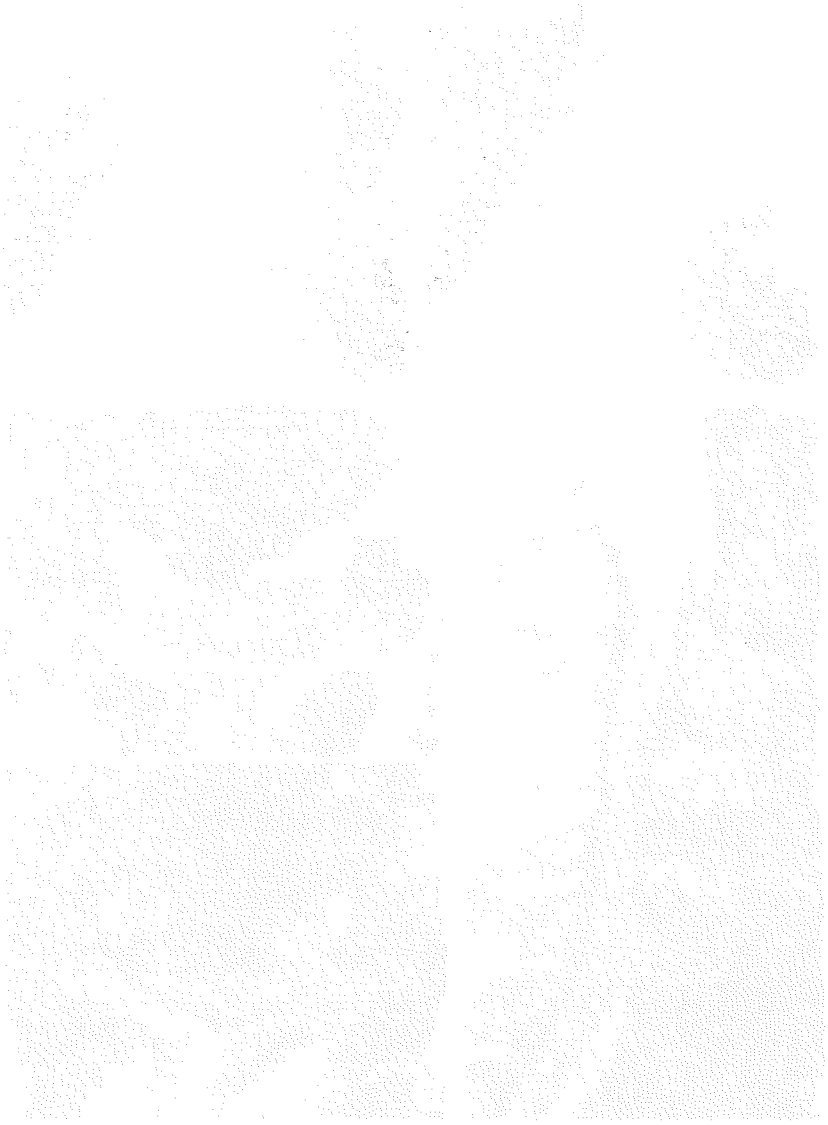

Eur Spine J (2010) 19:691–698
DOI 10.1007/s00586-009-1266-4

ORIGINAL ARTICLE

Posterior decompression with instrumented fusion for thoracic myelopathy caused by ossification of the posterior longitudinal ligament

Masashi Yamazaki · Akihiko Okawa · Takayuki Fujiyoshi · Takeo Furuya · Masao Koda

Received: 25 April 2009 / Revised: 19 October 2009 / Accepted: 23 December 2009 / Published online: 6 January 2010

Abstract We evaluated the clinical results of posterior decompression with instrumented fusion (PDF) for thoracic myelopathy due to ossification of the posterior longitudinal ligament (OPLL). A total of 24 patients underwent PDF, and their surgical outcomes were evaluated by the Japanese Orthopaedic Association (JOA) scores (0–11 points) and by recovery rates calculated at 3, 6, 9 and 12 months after surgery and at a mean final follow-up of 4 years and 5 months. The mean JOA score before surgery was 3.7 points. Although transient paralysis occurred immediately after surgery in one patient (3.8%), all patients showed neurological recovery at the final follow-up with a mean JOA score of 8.0 points and a mean recovery rate of 58.1%. The mean recovery rate at 3, 6, 9 and 12 months after surgery was 36.7, 48.8, 54.0 and 56.8%, respectively. The median time point that the JOA score reached its peak value was 9 months after surgery. No patient chose additional anterior decompression surgery via thoracotomy. The present findings demonstrate that despite persistent anterior impingement of the spinal cord by residual OPLL, PDF can result in considerable neurological recovery with a low risk of postoperative paralysis. Since neurological recovery progresses slowly after PDF, we suggest that additional anterior decompression surgery is not desirable during the early stage of recovery.

M. Yamazaki (✉) · A. Okawa · T. Fujiyoshi · T. Furuya · M. Koda
Spine Section, Department of Orthopaedic Surgery, Chiba University Graduate School of Medicine, 1-8-1 Inohana, Chuo-ku, Chiba 260-8677, Japan
e-mail: masashiy@faculty.chiba-u.jp

Keywords Thoracic myelopathy · Ossification of posterior longitudinal ligament · Kyphosis · Spinal mobility · Instrumented fusion

Introduction

Previous reports have shown that the results of surgery for thoracic myelopathy caused by ossification of the posterior longitudinal ligament (OPLL) unfavorably compare with results for cervical OPLL [12, 19]. Surgeons have employed a variety of surgical procedures to treat thoracic OPLL, including laminectomy [5], OPLL extirpation through thoracotomy [2, 4, 10], OPLL extirpation through a posterior approach [13], and circumspinal decompression [6, 15]. However, postoperative paraplegia remains a major risk [2, 4, 8–10, 13, 15]. At our institute, two patients experienced transient postoperative paraparesis after laminectomy, which resolved after the addition of posterior instrumented fusion without OPLL extirpation [16, 17]. On the basis of these two cases, we hypothesized that stabilizing the spine with instrumentation could yield a certain degree of neurological recovery even without complete OPLL extirpation. Based on this hypothesis, in 1989, we introduced the surgical procedure of posterior decompression with instrumented fusion (PDF) for patients with thoracic OPLL, in whom OPLL extirpation entailed a risk of neurological deterioration [18].

In an earlier series of ours, our patients enjoyed a considerable degree of neurological recovery following PDF despite persistent anterior impingement of the spinal cord by residual OPLL [18]. In addition, PDF was associated with an extremely low risk of postoperative paralysis and late neurological deterioration, compared with complication rates for laminectomy [5] and OPLL extirpation [2, 4].